

ON ONE DIMENSIONAL WEIGHTED POINCARÉ INEQUALITIES FOR GLOBAL SENSITIVITY ANALYSIS

DAVID HEREDIA, ALDÉRIC JOULIN, OLIVIER ROUSTANT

ABSTRACT. One-dimensional Poincaré inequalities are used in Global Sensitivity Analysis (GSA) to provide derivative-based upper bounds and approximations of Sobol indices. We add new perspectives by investigating weighted Poincaré inequalities. Our contributions are twofold. In a first part, we provide new theoretical results for weighted Poincaré inequalities, guided by GSA needs. We revisit the construction of weights from monotonic functions, providing a new proof from a spectral point of view. In this approach, given a monotonic function g , the weight is built such that g is the first non-trivial eigenfunction of a convenient diffusion operator. This allows us to reconsider the “linear standard”, *i.e.* the weight associated to a linear g . In particular, we construct weights that guarantee the existence of an orthonormal basis of eigenfunctions, leading to approximation of Sobol indices with Parseval formulas. In a second part, we develop specific methods for GSA. We study the equality case of the upper bound of a total Sobol index, and link the sharpness of the inequality to the proximity of the main effect to the eigenfunction. This leads us to theoretically investigate the construction of data-driven weights from estimators of the main effects when they are monotonic, another extension of the linear standard. Finally, we illustrate the benefits of using weights on a GSA study of two toy models and a real flooding application, involving the Poincaré constant and/or the whole eigenbasis.

CONTENTS

1. Introduction	2
1.1. Motivation	2
1.2. Contributions and plan	4
2. Background on weighted Poincaré inequalities	5
3. Main results on weighted Poincaré inequalities	8
3.1. A general result on the construction of weights	8
3.2. Revisiting the optimal weight for linear saturating functions	10
3.3. Beyond w_{lin} : non-vanishing weights on finite intervals	11
3.4. Numerical computation	12
3.5. When the weighted Poincaré inequality is not saturated	13
4. Link with global sensitivity analysis	19
4.1. Upper bounds for total Sobol indices	19
4.2. Case of equality in the upper bound and stability	20
4.3. Data-driven weights for monotonic main effects	21
4.4. Approximations of total Sobol indices with Poincaré chaos expansions	23
4.5. Summary and guidelines for choosing weights to GSA	25
5. Applications	25
5.1. Numerical settings	25

5.2. Illustration with toy models	26
5.3. Application to a flood model	29
Acknowledgement	32
Appendix A.	32
References	34

1. INTRODUCTION

1.1. Motivation

The development of Global Sensitivity Analysis (GSA) of numerical model outputs has become increasingly popular in the three last decades. It is by now an essential international research topic, combining modern mathematical and statistical tools to computer experiments, and has many consequences in engineering for industry. Recall that the principle of GSA is to quantify the influence of input random variables on the output of a multivariate function $f : \mathbb{R}^d \rightarrow \mathbb{R}$ which might be expensive to evaluate since dimension d is large. These variables can represent calculation codes that model complex phenomena or artificial intelligence algorithms whose functioning is not well understood.

When it comes to quantifying influence or uncertainty, practitioners tend to use Sobol indices [31, 32] because of their clear interpretation in terms of ANOVA decomposition, at least under the assumption of independent entries. More precisely, they are defined according to the Sobol Hoeffding decomposition

$$f(X) = \sum_{I \subset \{1, \dots, d\}} f_I(X_I),$$

where $X = (X_1, \dots, X_d)$ is the d -dimensional random vector of independent inputs X_i and provided the output random variable $f(X)$ lies in L^2 . Above each X_I is the random vector formed by the variables X_i with $i \in I$ and the terms $f_I(X_I)$ are uniquely characterized by the non-overlapping property

$$\mathbb{E}[f_I(X_I) | X_J] = 0, \quad \text{for all } J \subsetneq I,$$

where by convention $\mathbb{E}[\cdot | X_J] = \mathbb{E}[\cdot]$ when $J = \emptyset$. Such conditions imply the orthogonal decomposition of the total variance

$$\text{Var}(f(X)) = \sum_{I \subset \{1, \dots, d\}} \text{Var}(f_I(X_I)).$$

In particular, the main effects $f_i(X_i)$ carry the influence of each variable individually and the total contributions are captured by the total effects

$$f_i^{\text{tot}}(X) = \sum_{I \ni i} f_I(X_I).$$

2020 Mathematics Subject Classification. 26D10, 39B62, 37A30, 60J60, 62G05, 62P30, 65C60.

Key words and phrases. Weighted Poincaré inequality, spectral gap, Global Sensitivity Analysis, Sobol-Hoeffding decomposition, Sobol indices, weighted Derivative-based Global Sensitivity Measures, Poincaré chaos expansion.

The latter naturally defines total Sobol indices as the percentage of variance explained by them:

$$S_i^{\text{tot}} = \frac{\text{Var}(f_i^{\text{tot}}(X))}{\text{Var}(f(X))} \in [0, 1].$$

Despite their clear interpretability, the estimation of total Sobol indices requires numerous calculations, making them an expensive computational tool. When the derivatives of f are available, other sensitivity indices called DGSM (Derivative-based Global Sensitivity Measure) reveal to be efficient since they are cheaper to compute, cf. [33, 34]. As observed in [19] and further studied in detail in [26], Sobol indices and DGSM are connected by a one-dimensional Poincaré inequality. In other words, when it is satisfied, such a functional inequality provides an upper bound of the variance-based index by using the derivative-based one, easier to handle in practice. Hence DGSM indices can be seen as a credible alternative to Sobol indices for screening purposes, allowing to identify input variables with minimal influence when the devoted DGSM indices are sufficiently small (balanced with the other components appearing in the upper bound). To apply these techniques, providing some information on the Poincaré constant, *i.e.*, the best constant in the Poincaré inequality, is of crucial importance. Since in theory it is quite hard to find explicitly those objects even in our one-dimensional context, some numerical methods are required. As presented in [26], they are mainly based on a combination of the spectral interpretation of the Poincaré constant together with an appropriate finite element discretization which is relevant in the context of small dimension.

Actually, there is absolutely no reason to limit ourselves to bound from above Sobol indices only by DGSM ones, at least for two reasons. On the one hand there exists some usual probability measures which do not satisfy the usual Poincaré inequality (*e.g.*, heavy-tailed distributions) and on the other hand the DGSM-based upper bounds might be too large. To overcome this difficulty, we shall use another functional inequality involving the variance and alternative quantities still constructed with respect to the derivatives of the function f . Hence we are naturally led to introduce appropriate weight functions w_i in the DGSM indices. It gives rise to the notion of weighted DGSM indices

$$\nu_{i,w_i} = \mathbb{E} \left[w_i(X_i) \left(\frac{\partial f}{\partial x_i}(X) \right)^2 \right],$$

provided the expectation makes sense, the univariate dependence of the chosen weights being natural within the present one-dimensional context. Such functional inequalities are called weighted Poincaré inequalities and yield to the key upper bound

$$S_i^{\text{tot}} \leq C_P(\mu_i, w_i) \frac{\nu_{i,w_i}}{\text{Var}(f(X))},$$

where μ_i stands for the distribution of the input random variable X_i and the Poincaré constant $C_P(\mu_i, w_i)$ depends on the weight w_i (the unweighted case corresponding to the classical choice $w_i \equiv 1$). Hence it provides an additional degree of freedom by choosing conveniently the weight to enhance the precision of the upper bound. In particular it suggests, among other things, the construction of data-driven weights in order to improve the classical (unweighted) results offered in [26] when applied to specific models arising in the GSA methodology.

To conclude with motivations, notice that this framework is not limited to provide only upper bounds on Sobol indices. Indeed, under slightly additional assumptions, we may consider the spectral interpretation related to the weighted Poincaré inequalities, giving rise to the so-called Poincaré chaos, somewhat similar to that emphasized in [21, 27]. See also [1] for another usage of spectral expansions through Sturm-Liouville operators. Then, all Sobol indices can be expressed as Parseval identities and truncations of these identities give relevant derivative-based lower bounds on those indices. Here also, considering a weight in Poincaré inequalities provides an additional degree of freedom that should help to improve these lower bounds.

To illustrate the strength of weighted Poincaré inequalities in GSA, we provide in Figure 1 some numerical computations of total Sobol indices and associated estimated bounds on a GSA standard model (we refer to Section 5 for more details). We can see that, compared to the results of the unweighted case reported in [26], using weights clearly improves the accuracy of the upper and lower bounds.

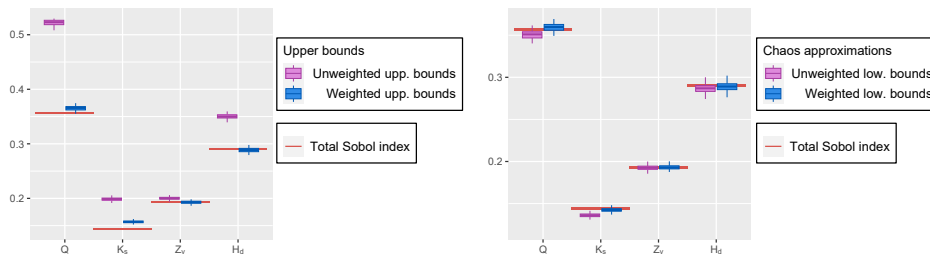


FIGURE 1. Illustration of the benefits of using weights in Poincaré inequalities for bounding total Sobol indices on the hydrological problem of Section 5.3.

1.2. Contributions and plan

The present work is divided into two main parts: first we provide new theoretical results for weighted Poincaré inequalities, driven by GSA needs, whereas in a second time we develop specific applications to GSA. Finally we illustrate numerically our results on toy models to observe the relevance of our approach and in particular on a flood model. Here is below a detailed description of our main contributions together with a plan of the paper.

Section 2 offers an introduction to theoretical aspects of weighted Poincaré inequalities and their corresponding spectral interpretation. Then our main contributions on these weighted functional inequalities are contained in Section 3. In a nutshell, they can be summarized as follows.

Firstly, we revisit the construction of weights presented in [15], offering a new proof from a spectral point of view and without requiring to the formalism of Stein's method. In addition, we provide a necessary and sufficient condition for obtaining non-vanishing weights. In this construction, given some suitable monotonic function g_i , we determine the weight w_i for which g_i is the first non-trivial eigenfunction of a convenient diffusion operator involving w_i as diffusion constant. As a result, g_i is essentially the only function to saturate the weighted Poincaré inequality. Furthermore, we provide a numerical method to approximate the weight w_i when it does not admit a closed-form expression, a situation encountered in GSA when the

distribution of the input variables are non-standard.

Secondly, we further investigate the common weight choice associated to the case where g_i is linear. This case was studied for GSA in [35] by means of a calculus of variations approach (Euler-Lagrange equations). We expand their list of weights by including several examples related to truncated or heavy-tailed probability measures. Beyond this standard, we propose a new way to construct non-vanishing weights, based on a reference probability measure.

Thirdly, we consider the case where the weighted Poincaré inequality is not saturated, *i.e.* when the first eigenfunction does not exist. Thanks to the intertwining approach proposed in [8, 9], we are able to provide the exact value of the Poincaré constant for original and new examples involving a large class of weights.

In Section 4, we develop GSA-oriented results and in particular data-driven weights. We study the equality case of the upper bound of a total Sobol index, linking the sharpness of the inequality to the proximity of the main effect f_i with respect to the eigenfunction g_i . This justifies the common weight choice associated to a linear g_i for models that exhibit almost linear main effects. But this also suggests the construction of data-driven weights from estimators of the main effects when they are monotonic (and not only linear). In some sense, this is a data-driven version of the general weight proposed in Section 3. We prove the consistency of this weight estimator and the associated upper bound.

Our final Section 5 is dedicated to applications. We collect all the previous material to study two toy models and a real flooding application, involving the Poincaré constant and/or the whole eigenbasis. In particular our numerical results on the flood model reveal to be relevant and exhibit a serious improvement of the ones established in [26] through the usual (*i.e.* unweighted) Poincaré inequalities and Poincaré chaos.

To conclude this introduction, we point out that our approach is limited to one-dimensional functional inequalities for the moment but it would be very natural to generalize our results to higher dimensions. A nice first result was presented in the recent article [13] in which the authors generalize the Stein approach to some multi-dimensional log-concave probability measures such as moment measures of convex functions. In some sense this work can be seen as a multi-dimensional extension of [15] by means of Stein kernel weights, and also of [35] although the methods emphasized are somewhat different. Nevertheless this generalization to higher dimension remains open in full generality and would have many challenging and interesting consequences from a GSA perspective since then high-dimensional independent inputs X_i with non necessarily independent coordinates could be addressed. We hope that such a direction will be the matter of future research.

2. BACKGROUND ON WEIGHTED POINCARÉ INEQUALITIES

We start by briefly introducing some theoretical aspects about one-dimensional weighted Poincaré inequalities, which are the main protagonists of the present paper.

Given $-\infty \leq a < b \leq \infty$, we denote by $\mathcal{C}_+^{0,1}(a, b)$ the set of functions that are continuous and piecewise \mathcal{C}^1 (*i.e.* continuously differentiable) on $[a, b]$ and positive on (a, b) . We define $\mathcal{C}_*^{1,2}(a, b)$ as the class of functions f such that $f' \in \mathcal{C}_+^{0,1}(a, b)$ or $-f' \in \mathcal{C}_+^{0,1}(a, b)$. We denote $\mathcal{P}(a, b)$ the set of probability measures μ on $[a, b]$ with density (with respect to the Lebesgue measure) $\rho \in \mathcal{C}_+^{0,1}(a, b)$ satisfying $\rho(a) > 0$

(resp. $\rho(b) > 0$) when a (resp. b) is finite. Let $\mathcal{W}(a, b)$ be the set of continuous functions on $[a, b]$, that are piecewise \mathcal{C}^1 and positive on (a, b) . In the sequel we systematically refer to functions $w \in \mathcal{W}(a, b)$ as weights. Note that $\mathcal{W}(a, b)$ differs from $\mathcal{C}_+^{0,1}(a, b)$ since we do not require weights to be differentiable at the boundaries. In the case where a and/or b are infinite, we adopt the convention $[-\infty, b] = (-\infty, b]$ and/or $[a, \infty] = [a, \infty)$, to avoid making the distinction every time. It is of course possible to consider a more general setting, but this one is relevant and fulfills our purposes.

Let $L^2(\mu)$ be the space of square-integrable functions with respect to some probability measure $\mu \in \mathcal{P}(a, b)$ and, given some weight function $w \in \mathcal{W}(a, b)$, denote $H^1(\mu, w)$ the weighted Sobolev space defined as

$$H^1(\mu, w) = \left\{ f \in L^2(\mu) \mid w^{1/2} f' \in L^2(\mu) \right\},$$

where f' stands for the weak derivative of the function f . We are now in position to give the definition of a weighted Poincaré inequality.

Definition 2.1. *A probability measure $\mu \in \mathcal{P}(a, b)$ satisfies a weighted Poincaré inequality with weight function $w \in \mathcal{W}(a, b)$ and constant $C > 0$ if for every function $f \in H^1(\mu, w)$ such that $\int_a^b f d\mu = 0$ (we say that f is centered), it is true that*

$$\int_a^b f^2 d\mu \leq C \int_a^b w (f')^2 d\mu. \quad (2.1)$$

The Poincaré constant, denoted $C_P(\mu, w)$, is the optimal (i.e., the smallest) constant C for which (2.1) holds. If there exists some non-null function which realizes the equality in (2.1), we say that it saturates the weighted Poincaré inequality.

In the particular case where $w \equiv 1$, we are reduced to the classical Poincaré inequality which has been largely studied in the literature. See for instance [2] for an introduction to the topic, with precise references and credit.

Actually, such an idea to consider weighted functional inequalities of Poincaré type takes roots at least in the 70s within the pioneer work of Brascamp and Lieb [10] in a multi-dimensional log-concave context. Moreover it reveals to have strong consequences in high-dimensional analysis, in connection with other important functional inequalities, isoperimetry and concentration of measure, cf. for instance the work of Bobkov and Ledoux [7] about general convex measures including heavy-tailed distributions, i.e., probability distributions whose tails decay is slower than exponential. In the one-dimensional case, the analysis can be further explored either by considering Hardy-type inequalities and Sturm-Liouville equations [4, 5, 22] or using Stein's method as in the papers [15, 29] in which the weight corresponds to the so-called Stein kernel. Recently, new theoretical guarantees have been proposed in [8, 9] by means of the intertwining technique. Such an approach will be developed in Section 3.5.

Similarly to the usual one $C_P(\mu, 1)$, the Poincaré constant $C_P(\mu, w)$ admits a dual interpretation related to a convenient diffusion operator. To observe this, we need to introduce a bit of structure. Denote $\mathcal{C}^\infty(a, b)$ the space of infinitely differentiable real-valued functions on $[a, b]$ and consider the subspace

$$\mathcal{C}_{N,w}^\infty(a, b) = \{f \in \mathcal{C}^\infty(a, b) \mid w(a)f'(a)\rho(a) = w(b)f'(b)\rho(b) = 0\},$$

the presence of the index N standing for Neumann boundary conditions adapted to the presence of the weight w (these are the only boundary conditions we will

consider throughout this paper). If a and/or b are infinite, the boundary conditions above are understood as taking the limit $a \rightarrow -\infty$ and/or $b \rightarrow \infty$. Then the diffusion operator of interest is defined on $\mathcal{C}_{N,w}^\infty(a, b)$ as follows:

$$L_w f = \frac{1}{\rho} (w f' \rho)' = w f'' + (w' + w(\log \rho)') f'.$$

Note that this operator involves the weight w as diffusion constant, in contrast to the canonical operator usually related to the probability measure μ , *i.e.*, the one constructed with the choice $w \equiv 1$. Trivial integrations by parts tell us that the operator $-L_w$ is symmetric on $\mathcal{C}_{N,w}^\infty(a, b) \subset L^2(\mu)$ and non-negative, *i.e.*, for every $f, g \in \mathcal{C}_{N,w}^\infty(a, b)$,

$$\int_a^b (-L_w f) g \, d\mu = \int_a^b w f' g' \, d\mu = \int_a^b f (-L_w g) \, d\mu,$$

and

$$\int_a^b (-L_w f) f \, d\mu = \int_a^b w (f')^2 \, d\mu \geq 0, \quad (2.2)$$

respectively. If $[a, b]$ is finite and w does not vanish at the boundary, the operator is said to be regular according to the formalism of Sturm-Liouville problems and it is essentially self-adjoint in $L^2(\mu)$, *i.e.*, it admits a unique self-adjoint extension (still denoted $-L_w$) with domain $\mathcal{D}(-L_w) \subset L^2(\mu)$ in which the space $\mathcal{C}_{N,w}^\infty(a, b)$ is dense for the operator norm. Otherwise the operator is called singular and to ensure this essentially self-adjointness property, the metric induced by the operator (or rather by the so-called *carré du champ* operator, thus by w) is assumed to be complete. We refer to [36] for a classical reference about Sturm-Liouville problems and to Chapter 3 of [2] for the essentially self-adjointness property studied in the context of general diffusion Markov triples.

Once the (unique) self-adjoint extension is defined, let us introduce some elements about the eigenvalues and eigenfunctions of the operator $-L_w$. Roughly speaking, the eigenvalues correspond to a part of the spectrum $\sigma(-L_w) \subset \mathbb{R}^+$ given by the values λ for which there exists a centered function $g \in \mathcal{D}(-L_w)$ satisfying $-L_w g = \lambda g$, *i.e.*, an eigenfunction associated to λ . Note that our definition of eigenvalue differs a bit from the usual definition since λ may not be isolated. In the present context, the first eigenvalue is $\lambda_0(-L_w) = 0$ and the associated one-dimensional eigenspace is generated by the constant eigenfunction $e_0 \equiv 1$. If 0 is isolated in the spectrum, it means that the second element of the spectrum defined by the variational formula

$$\lambda_1(-L_w) = \inf_{\substack{f \in H^1(\mu, w) \\ f \text{ centered}}} \frac{\int_a^b (-L_w f) f \, d\mu}{\int_a^b f^2 \, d\mu}, \quad (2.3)$$

is positive. The quantity $\lambda_1(-L_w)$ ($= \lambda_1(-L_w) - \lambda_0(-L_w)$) is called the spectral gap of the diffusion operator $-L_w$. Note that it may not be an eigenvalue since the infimum above is not always reached. Using (2.2), we deduce that the Poincaré constant $C_P(\mu, w)$ admits the following spectral interpretation:

$$C_P(\mu, w) = \frac{1}{\lambda_1(-L_w)}.$$

In this way, finding the Poincaré constant $C_P(\mu, w)$ is equivalent to identify the spectral gap $\lambda_1(-L_w)$, a dual interpretation which will be systematically used in

our paper. Moreover, if the eigenspace related to the spectral gap is non empty, it is also one-dimensional and a given function e_1 (say) is an associated eigenfunction if and only if it saturates the weighted Poincaré inequality (2.1). In particular it satisfies for all $g \in H^1(\mu, w)$,

$$\int_a^b g e_1 d\mu = C_P(\mu, w) \int_a^b g (-L_w e_1) d\mu = C_P(\mu, w) \int_a^b w g' e_1' d\mu. \quad (2.4)$$

To finish this introduction about weighted Poincaré inequalities, we point out that it is a difficult task in general to give the explicit value of the spectral gap, except maybe for some particular examples of probability measures and weights. However there exists a useful method in the present one-dimensional setting which allows to identify it when the eigenfunction e_1 exists. By [12] we know that e_1 is the only eigenfunction of the operator $-L_w$ such that its derivative does not vanish on (a, b) , is of constant sign and satisfies $w(a)f'(a)\rho(a) = w(b)f'(b)\rho(b) = 0$. In other words, if we find some eigenfunction satisfying these properties, then the associated eigenvalue is necessarily the spectral gap. Actually, this observation is the main idea behind our main results to which we turn now.

3. MAIN RESULTS ON WEIGHTED POINCARÉ INEQUALITIES

3.1. A general result on the construction of weights

In this part, we revisit the formulation of the optimal weight built by means of the Stein method in [14, Theorem 3.5] (with $l = 0$) and in [15, Theorem 2.4], offering a new proof from a spectral point of view. In other words, Theorem 3.1 below determines the weight for which a suitably selected function saturates the weighted Poincaré inequality. In particular this result extends the weights provided in [35] with linear saturating functions.

Notice that each weight and corresponding Poincaré constant are uniquely defined up to a multiplicative constant since $C_P(\mu, kw) = k^{-1}C_P(\mu, w)$ for every $k > 0$. In this section we adopt the normalization $C_P(\mu, w) = 1$.

Theorem 3.1. *Let $\mu \in \mathcal{P}(a, b)$ and let g be a centered function in $\mathcal{C}_*^{1,2}(a, b)$. If a (resp. b) is finite we assume that $g'(a) \neq 0$, or that $g'(a) = 0$ and $g''(a) \neq 0$ (resp. $g'(b) \neq 0$, or that $g'(b) = 0$ and $g''(b) \neq 0$). Then*

- The function

$$w_g(x) = -\frac{1}{g'(x)\rho(x)} \int_a^x g(y)\rho(y) dy, \quad x \in (a, b), \quad (3.1)$$

belongs to $\mathcal{W}(a, b)$. If a is finite, the value of $w_g(a)$ depends on g :

- If $g'(a) \neq 0$, then $w_g(a) = 0$.
- If $g'(a) = 0$ and $g''(a) \neq 0$, then $w_g(a) = -g(a)/g''(a) > 0$.

The same conclusion holds for $w_g(b)$ if b is finite.

- If in addition $g \in L^2(\mu)$ (which is satisfied if a and b are finite), then the weighted Poincaré inequality (2.1) holds with weight w_g and Poincaré constant $C_P(\mu, w_g) = 1$. Furthermore, the inequality is saturated by g .

Proof. We start dealing with the regularity of our weight. The definition of w_g in (3.1) provides its continuity on (a, b) . We multiply by $g'\rho$ in both sides and differentiate to obtain

$$(w_g g' \rho)' = -g\rho, \quad (3.2)$$

so that we get on (a, b) ,

$$w'_g = -\frac{g}{g'} - w_g \left(\frac{g''}{g'} + \frac{\rho'}{\rho} \right).$$

Then, the regularity of g and ρ together with the fact that g' and ρ do not vanish on (a, b) show that w'_g is piecewise continuous and thus w_g is piecewise \mathcal{C}^1 on (a, b) .

Let us prove now that w_g is positive on (a, b) . The function g is centered and increasing, hence $\lim_{x \rightarrow a} g(x) < 0$, $\lim_{x \rightarrow b} g(x) > 0$ and there exists a unique $c \in (a, b)$ such that $g(c) = 0$. Denoting $G(x) := \int_a^x g(y)\rho(y) dy$, $x \in (a, b)$, we have the following table:

	a	c	b
G'	-	0	+
G	↘		↗

and since $\lim_{x \rightarrow a} G(x) = \lim_{x \rightarrow b} G(x) = 0$, we obtain $G < 0$ and thus $w_g > 0$ on (a, b) .

Next, if a is finite the value $w_g(a)$ is defined as the limit of $w_g(x)$ when $x \rightarrow a$, guaranteeing its right-continuity at point a (the value $w_g(b)$ is obtained identically when b is finite, providing the left-continuity at b). Namely if $g'(a) \neq 0$, then we observe immediately from the definition of w_g that $w_g(a) = 0$. Otherwise if $g'(a) = 0$ and $g''(a) \neq 0$, then we rewrite w_g as

$$w_g(x) = -\frac{x-a}{(g'(x) - g'(a))\rho(x)} \times \frac{1}{x-a} \int_a^x g(y)\rho(y) dy, \quad x \in (a, b),$$

so that taking the limit $x \rightarrow a$ entails that $w_g(a) = -g(a)/g''(a)$.

Finally, to prove that the weighted Poincaré inequality (2.1) is satisfied with weight w_g and Poincaré constant $C_P(\mu, w_g) = 1$ when $g \in L^2(\mu)$, we consider the spectral interpretation of the Poincaré constant. Equality (3.2) indicates that g is an eigenfunction of (minus) the operator

$$L_{w_g} f = \frac{(w_g f' \rho)'}{\rho},$$

with associated eigenvalue $\lambda = 1$. Furthermore, since the derivative of g does not vanish on (a, b) , then the spectral gap $\lambda_1(-L_{w_g})$ coincides necessarily with this eigenvalue, meaning that

$$C_P(\mu, w_g) = \frac{1}{\lambda_1(-L_{w_g})} = 1,$$

and that the weighted Poincaré inequality is saturated by g . The proof of Theorem 3.1 is now complete. \square

Notice that the assumptions on g in Theorem 3.1 mimic the properties required to be an eigenfunction e_1 associated to the inverse Poincaré constant. Indeed, first we know that e_1 is centered and is the only eigenfunction (up to a multiplicative constant) of the operator $-L_{w_g}$ satisfying $e'_1 > 0$ (up to a change of sign). Secondly, if $[a, b]$ is a finite interval, the possible boundary conditions are consistent with the values of w_g at the boundary (we have $w_g(a)g'(a)\rho(a) = w_g(b)g'(b)\rho(b) = 0$) and prevent it from exploding.

As we will see in the sequel, Theorem 3.1 is one of the result on which our forthcoming numerical study is based and thus will be used many times in our paper, in particular when dealing with applications to GSA. When the weight w_g provided by (3.1) does not admit a closed-form expression, we will implement a numerical method that approximates it for any suitable pair of probability measure μ and function g . This method is further detailed in Section 3.4. Before that, let us revisit the classical situation where g is a linear function and investigate new relevant weights provided by Theorem 3.1.

3.2. Revisiting the optimal weight for linear saturating functions

The classical weight w_{lin} (say) used in the literature corresponds in Theorem 3.1 to the linear choice

$$g(x) = g_{\text{lin}}(x) = x - \int_a^b y \rho(y) dy,$$

which is often convenient since linear functions saturate the devoted weighted Poincaré inequality. This weight is given by the formula

$$w_{\text{lin}}(x) = -\frac{1}{\rho(x)} \int_a^x g_{\text{lin}}(y) \rho(y) dy, \quad x \in [a, b].$$

In particular we will see in Section 4.2 that this choice is optimal when approximating linear phenomena in the GSA context. Notice that w_{lin} has to vanish at the boundary (if non empty) since $g'_{\text{lin}} \equiv 1$ does not vanish at the boundary. Following this strategy, the authors in [35] give a list of closed-form expressions for w_{lin} associated to classical laws, including the uniform, exponential and Gaussian distributions.

However it is necessary to consider other examples frequently encountered in GSA problems, typically truncated distributions. Heavy-tailed measures are also considered, for which the presence of a weight becomes necessary to establish a Poincaré-type inequality (recall that they do not satisfy the classical one due to the lack of exponential integrability, see for instance [2]). Table 1 below provides some of those examples, including two heavy-tailed distributions: the generalized Cauchy measure μ_β of parameter $\beta > 1/2$, denoted $\mathcal{C}(\beta)$, whose density is defined as

$$\rho(x) = \frac{1}{Z_\beta (1+x^2)^\beta}, \quad x \in \mathbb{R},$$

with Z_β the normalization constant, and the Pareto distribution $\mu_{z,\alpha}$ with parameters $z > 0$ and $\alpha > 0$, denoted $\mathcal{P}ar(z, \alpha)$, with density given by

$$\rho(x) = \frac{\alpha z^\alpha}{x^{\alpha+1}}, \quad x \geq z.$$

According to Theorem 3.1, both measures satisfy a weighted Poincaré inequality with their respective weights w_{lin} if they admit a finite second moment. This condition is fulfilled when $\beta > 3/2$ and $\alpha > 2$, respectively. Table 1 also includes the exact expression of the weight w_{lin} for some truncated probability measures. We refer to Appendix A for detailed computations. All the weights vanish at the boundary (when non empty), as expected according to Theorem 3.1. Moreover they converge pointwise as $h \rightarrow \infty$ to the weight w_{lin} on the whole space (provided it is well-defined, *i.e.* g_{lin} is square-integrable), a property which is also true in full generality. Regarding the truncated versions of $\mathcal{C}(\beta)$ and $\mathcal{P}ar(z, \alpha)$, we point

out that the parameters β and α can take any real value since the Lebesgue density is always continuous on the truncated interval and thus no extra integrability condition is required.

Probability measure μ	Weight w_{lin}	
Uniform $\mathcal{U}(a, b)$	$\frac{1}{2}(x-a)(b-x)$	
Exponential $\mathcal{E}(\gamma)$	On \mathbb{R}^+	Truncated on $[0, h]$
	$\frac{x}{\gamma}$	$\frac{1}{\gamma} \left(x - h \frac{1 - e^{\gamma x}}{1 - e^{\gamma h}} \right)$
Normal $\mathcal{N}(m, \sigma^2)$	On \mathbb{R}	Truncated on $[m-h, m+h]$
	σ^2	$\sigma^2 \left(1 - \exp \left(\frac{(x-m)^2}{2\sigma^2} - \frac{h^2}{2\sigma^2} \right) \right)$
Gen. Cauchy $\mathcal{C}(\beta)$	On \mathbb{R}	Truncated on $[-h, h]$
	For $\beta > 3/2$: $\frac{1+x^2}{2(\beta-1)}$	For $\beta \neq 1$: $\frac{1}{2(\beta-1)} \left((1+x^2) - (1+x^2)^\beta (1+h^2)^{-\beta+1} \right)$ For $\beta = 1$: $\frac{1}{2} (1+x^2) \log \left(\frac{1+h^2}{1+x^2} \right)$
Pareto $\mathcal{P}ar(z, \alpha)$	On $[z, \infty)$	Truncated on $[z, z+h]$
	For $\alpha > 2$: $\frac{x(x-z)}{\alpha-1}$	For $\alpha \neq 1$: $\frac{x^{\alpha+1}}{\alpha-1} \left(\frac{z^{1-\alpha} - (z+h)^{1-\alpha}}{z^{-\alpha} - (z+h)^{-\alpha}} (z^{-\alpha} - x^{-\alpha}) - (z^{1-\alpha} - x^{1-\alpha}) \right)$ For $\alpha = 1$: $x^2 \left(\log \left(\frac{z+h}{z} \right) \frac{z^{-1} - x^{-1}}{z^{-1} - (z+h)^{-1}} - \log \left(\frac{x}{z} \right) \right)$

TABLE 1. Examples of weight w_{lin} .

3.3. Beyond w_{lin} : non-vanishing weights on finite intervals

Theorem 3.1 allows the generation of weights with saturating functions beyond linear ones. Furthermore, it enables to consider non-vanishing weights. This case is particularly relevant in GSA since then the existence of an orthonormal basis of eigenfunctions is guaranteed, at least when the interval $[a, b]$ is finite (the associated Sturm-Liouville problem is regular, cf. [36]).

According to Theorem 3.1, adding the requirement that the desired weight does not vanish forces the associated saturating function g to satisfy very specific conditions. Namely, in addition to be a centered function in $\mathcal{C}_*^{1,2}(a, b)$, g must verify

$$g'(a) = g'(b) = 0, \quad g''(a) \neq 0 \quad \text{and} \quad g''(b) \neq 0. \quad (3.3)$$

A simple way to build such a suitable function is to consider another “reference” probability measure $\tilde{\mu}$ and to look at a function \tilde{g} saturating the corresponding classical Poincaré inequality. Indeed, \tilde{g} is an eigenfunction for the diffusion operator related to $\tilde{\mu}$ with (non-vanishing) constant weight equal 1, so that $\tilde{g} \in \mathcal{C}_*^{1,2}(a, b)$ and satisfies the Neumann conditions $\tilde{g}'(a) = \tilde{g}'(b) = 0$. It is easy to deduce that \tilde{g} then also verifies $\tilde{g}''(a) = \tilde{g}''(b) = 0$. The function g is then obtained by centering \tilde{g} with respect to μ . We collect all these elements in the following proposition.

Proposition 3.1. *Consider two probability measures $\mu, \tilde{\mu} \in \mathcal{P}(a, b)$ with (a, b) finite. Let \tilde{g} be the function saturating the classical Poincaré inequality for $\tilde{\mu}$. Then the function g defined by $g(x) = \tilde{g}(x) - \int_a^b \tilde{g}(y) \mu(dy)$ belongs to $\mathcal{C}_*^{1,2}(a, b)$ and*

satisfies (3.3). Moreover it generates a non-vanishing weight $w_g \in \mathcal{W}(a, b)$ leading to a weighted Poincaré inequality for μ .

There are several ways to define $\tilde{\mu}$. First, as an extension of w_{lin} , we can define $\tilde{\mu}$ on the finite interval $[a, b]$ for which \tilde{g} is close to be linear. In the context of GSA, the associated weight will be adapted to linear phenomena (as it is the case with w_{lin}), as explained by the stability argument given in Section 4.2. Since the function g_{lin} saturates the classical Poincaré inequality for the normal distribution on the real line, the idea is to choose $\tilde{\mu}$ as a truncated Gaussian measure highly concentrated in $[a, b]$. For instance, we consider for $\tilde{\mu}$ the distribution $\mathcal{N}\left(\frac{a+b}{2}, \sigma^2\right)|_{[a,b]}$, with variance σ^2 chosen such that $\mathbb{P}\left(\mathcal{N}\left(\frac{a+b}{2}, \sigma^2\right) \in [a, b]\right) = 0.95$. Then the corresponding function \tilde{g} is the so-called Kummer function given in terms of an hypergeometric series, see for instance [26]. As expected, numerical computations suggest that \tilde{g} is approximately linear except near the boundary since its derivatives vanish at these points. In the sequel, we denote by w_G the weight w_g associated to this choice of $\tilde{\mu}$ (by Proposition 3.1) in order to emphasize the role of the Gaussian distribution.

Secondly, another idea is to choose a convenient reference probability measure $\tilde{\mu}$ that allows simple computations. A natural candidate is the uniform distribution $\mathcal{U}(a, b)$. It is well-known that the optimal constant in the classical Poincaré inequality is $C_P(\tilde{\mu}, 1) = (b - a)^2/\pi^2$ and the corresponding saturating function is $\tilde{g}(x) = \cos(\pi(x - a)/(b - a))$. We note w_U the generated weight.

3.4. Numerical computation

In this short part we provide a numerical method to approximate the weight w_g from any eligible probability measure $\mu \in \mathcal{P}(a, b)$, with $[a, b]$ finite, and function g . The idea is to solve the Cauchy problem

$$\begin{cases} (w_g g' \rho)'(x) = -g(x)\rho(x) & \text{on } (a, b), \\ (w_g g' \rho)(a) = 0, \end{cases}$$

and then simply divide the solution by $g' \rho$. Above ρ stands for the Lebesgue density of μ . The method is implemented using the R software. To solve the differential equation we use the Runge-Kutta 4 method (in R, the function `rk4` from the package `deSolve` [30]) which is very accurate. Indeed, it is known that if h denotes the size of the uniform partition of the interval $[a, b]$, the approximation error at any point is of order $O(h^4)$, cf. for instance [11]. Note that the estimated weight vanishes at points a and b . To prevent inconsistencies when $w_g(a) \neq 0$ or/and $w_g(b) \neq 0$, we apply smooth corrections near the boundaries. We illustrate the precision of the numerical method by computing weights for the standard uniform distribution and a truncated normal one. Figures 2 and 3 below display the theoretical weights w_{lin} , together with their numerical approximations and the numerical approximations of w_U and w_G . To compute w_G , we initially approximate the function that generates it. This is carried out through the finite element method as in [26]. Note that for the case of the uniform distribution, w_U takes the constant value $C_P(\mu, 1) = 1/\pi^2$ (so that the probability measure μ and the reference one $\tilde{\mu}$ are the same).

Finally, Figure 4 below shows the numerical approximations of w_{lin} , w_G and w_U associated to a truncated Gumbel distribution that naturally appears in hydrology according to extreme value theory (its Lebesgue density is given in Section 5.3). We do not have a close expression for any of the weights in this case.

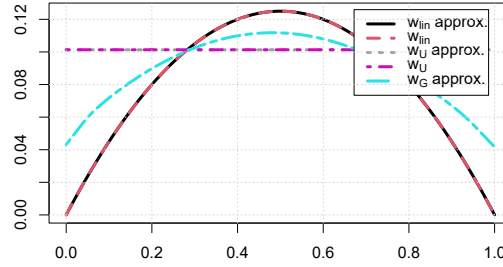


FIGURE 2. The weights $w_{\text{lin}}(x) = \frac{1}{2}x(1-x)$, $w_{\text{U}}(x) = 1/\pi^2$, their numerical approximations and the numerical approximation of w_{G} , associated to the uniform distribution $\mathcal{U}(0,1)$.

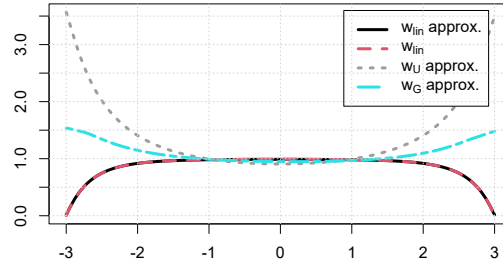


FIGURE 3. The weight $w_{\text{lin}}(x) = 1 - \exp(x^2/2 - 9/2)$, its numerical approximation and the numerical approximations of w_{U} and w_{G} , associated to the truncated normal distribution $\mathcal{N}(0,1)$ on the interval $[0,3]$.

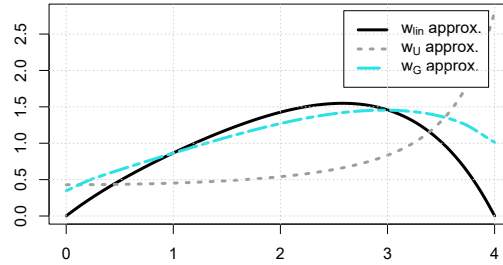


FIGURE 4. Numerical approximations of w_{lin} , w_{U} and w_{G} associated to the truncated Gumbel distribution $\mathcal{G}(0,1)$ truncated on $[0,4]$.

3.5. When the weighted Poincaré inequality is not saturated

As we have seen previously in Theorem 3.1, our strategy is to construct a weight such that the functions saturating the corresponding weighted Poincaré inequality can be identified. In other words, those functions are the eigenfunctions with associated eigenvalue the spectral gap, *i.e.*, the inverse Poincaré constant, of a convenient diffusion operator. However, two obstructions may occur within this framework: on the one hand the weight may not be explicitly computable and on the other

hand enforcing the existence of those saturating functions reduces drastically the scope of admissible weights. For instance the latter approach fails when considering linear functions associated to w_{lin} as in Section 3.2, which are not always square integrable with respect to heavy-tailed distributions.

In this part, we compute explicitly the Poincaré constant for more general weights. In particular we have in mind some examples for which the weighted Poincaré inequality does not admit saturating functions, so that Theorem 3.1 cannot be applied. To address this problem, the approach we adopt is based on the intertwining technique emphasized in [8, 9] in the one-dimensional case. Recall that a given probability measure $\mu \in \mathcal{P}(a, b)$ has density $\rho \in \mathcal{C}_+^{0,1}(a, b)$ which takes positive values at the boundary and the notation L_w stands for the (self-adjoint extension of the) operator defined on $\mathcal{C}_{N,w}^\infty(a, b)$ by

$$L_w f = w f'' + (w' + w(\log \rho)') f',$$

where $w \in \mathcal{W}(a, b)$ is a weight function.

Let us state first Theorem 4.2 in [8] but adapted to the present context.

Theorem 3.2. *Assume that there exists some smooth function h with non vanishing derivative on (a, b) such that the function*

$$M_{w,h} := \frac{(-L_w h)'}{h'}, \quad (3.4)$$

is bounded from below on (a, b) by some positive constant. Then we have the following weighted Poincaré inequality: for every centered function $f \in H^1(\mu, w)$,

$$\int_a^b f^2 d\mu \leq \int_a^b \frac{w (f')^2}{M_{w,h}} d\mu.$$

In particular it holds

$$C_P(\mu, w) \leq \frac{1}{\inf_{(a,b)} M_{w,h}}. \quad (3.5)$$

The formula (3.5) can be seen as a generalization to the operator L_w with diffusion constant w of the famous Chen-Wang result [12] on the spectral gap established by a coupling technique. As such, it has already been used in the Gaussian and generalized Cauchy cases to derive the exact expression of the Poincaré constants for some specific weights when there is no saturating function for the underlying weighted Poincaré inequalities, cf. [9] (in the generalized Cauchy case, it corresponds to parameters $\beta \in (1/2, 3/2]$, the range $\beta > 3/2$ being recovered directly in Table 1). In particular, an interesting choice of functions h (or rather h' since only h' and its derivatives appears in the formula) parametrized by $\varepsilon \in \mathbb{R}$ is $h'_\varepsilon = \rho^{-\varepsilon}/w$ so that we have on (a, b) ,

$$M_{w,\varepsilon} := M_{w,h_\varepsilon} = (1 - \varepsilon) w \left(\varepsilon ((\log \rho)')^2 - (\log \rho)'' \right). \quad (3.6)$$

Then by (3.5) we obtain

$$C_P(\mu, w) \leq \frac{1}{\sup_{\varepsilon \in \mathbb{R}} \inf_{(a,b)} M_{w,\varepsilon}}. \quad (3.7)$$

On the one hand when the weight is prescribed *a priori*, the estimate (3.7) is convenient in many situations. On the other hand when we look also at some convenient weight w , we proceed as follows: compute first the right-hand-side of (3.6)

(without w) which is expected to be non-negative for some relevant parameter ε , and then choose the desired weight w in such way that $M_{w,\varepsilon}$ is bounded from below by some positive constant c . If for some reasons we suspect that $c = C_P(\mu, w)$, then we try to find some sequence of centered functions (f_η) in $H^1(\mu, w)$, indexed by some parameter η , such that the Rayleigh quotient $\int_a^b f_\eta^2 d\mu / \int_a^b w (f'_\eta)^2 d\mu$ converges to c as η converges to some key value η^* . In practice the sequence (f_η) and the key value η^* are chosen such that the limiting function does not belong to $H^1(\mu, w)$.

As announced, let us observe what happens in some classical and less classical examples, for which we are able to derive the exact value of the Poincaré constant although there is no function saturating the weighted Poincaré inequality.

Example 3.1. Considering the exponential distribution μ_γ with parameter $\gamma > 0$, whose density is given on \mathbb{R}^+ by $\rho(x) = \gamma e^{-\gamma x}$, we have seen in Section 3.3 that the choice $w(x) = w_{\text{lin}}(x) = x/\gamma$ is related to linear eigenfunctions of the so-called Laguerre operator and yields $C_P(\mu_\gamma, w_{\text{lin}}) = 1$, see for instance [2]. In the unweighted case, there is no function saturating the Poincaré inequality, although we are able to identify the corresponding Poincaré constant: by [6], it is well known that $C_P(\mu_\gamma, 1) = 4/\gamma^2$ (from a spectral point of view, it corresponds to the bottom of the essential spectrum of the deviated operator) and the classical approach to obtain the inequality $C_P(\mu_\gamma, 1) \leq 4/\gamma^2$ uses a specific integration by part formula satisfied by μ_γ . Here we are able to recover the same bound directly with (3.7). Indeed, in this case the function $M_{1,\varepsilon}$ is constant on $(0, \infty)$ and has the value $\gamma^2\varepsilon(1 - \varepsilon)$. Optimizing with respect to ε yields

$$C_P(\mu_\gamma, 1) \leq \frac{1}{\sup_{\varepsilon \in \mathbb{R}} \gamma^2 \varepsilon (1 - \varepsilon)} = \frac{4}{\gamma^2}.$$

The converse inequality is proved by considering a family of centered functions $f_\eta(x) = e^{\eta x} - \gamma/(\gamma - \eta)$, with $\eta < \gamma/2$ so they belong to $H^1(\mu_\gamma, 1)$: we have after some computations,

$$\frac{\int_0^\infty f_\eta^2 d\mu_\gamma}{\int_0^\infty (f'_\eta)^2 d\mu_\gamma} = \frac{(\eta - \gamma)^2 - \gamma(\gamma - 2\eta)}{\eta^2(\eta - \gamma)^2},$$

and taking above the limit $\eta \rightarrow \gamma/2$ entails by (2.3) the inequality $C_P(\mu_\gamma, 1) \geq 4/\gamma^2$.

Example 3.2. In a somewhat similar unweighted context, we consider the generalized logistic (or skew-logistic) distribution μ_α of parameter $\alpha > 0$ on \mathbb{R} , namely with Lebesgue density

$$\rho(x) = \frac{\alpha e^{-x}}{(1 + e^{-x})^{\alpha+1}}, \quad x \in \mathbb{R}.$$

Similarly to the previous example, this probability measure is also log-concave on the real line, *i.e.*, $-\log \rho$ is a convex function on \mathbb{R} . When $\alpha = 1$ we deal with the classical logistic distribution, which can be seen as a regularized version around the origin of the Laplace distribution on the real line since $\rho(x) \sim e^{-|x|}$ as $|x| \rightarrow \infty$. In this case, the authors in [3] proved that $C_P(\mu_1, 1) = 4$ but there is no corresponding function saturating the Poincaré inequality. Let us recover this value from (3.7) and even prove that $C_P(\mu_\alpha, 1) = 4/\alpha^2$ for all $\alpha \in (0, 1]$ (the case $\alpha > 1$ could be

addressed as well, but we are only able to find the bounds $4/\alpha^2 \leq C_P(\mu_\alpha, 1) \leq 4$, as suggested by the computations below). Given some $\varepsilon \in \mathbb{R}$, we have for all $x \in \mathbb{R}$,

$$M_{1,\varepsilon}(x) = \varepsilon(1 - \varepsilon) + \frac{1 - \varepsilon}{(1 + e^x)^2} \left((\alpha + 1)(1 - 2\varepsilon)e^x + \varepsilon(\alpha^2 - 1) \right).$$

Choosing $0 \leq \varepsilon \leq 1/2$ entails that $M_{1,\varepsilon}$ starts being increasing, then reaches its maximum and becomes decreasing. In particular this implies that

$$\inf_{x \in \mathbb{R}} M_{1,\varepsilon}(x) = \min \left\{ \lim_{x \rightarrow -\infty} M_{1,\varepsilon}(x), \lim_{x \rightarrow \infty} M_{1,\varepsilon}(x) \right\} = \varepsilon(1 - \varepsilon) \min\{\alpha^2, 1\} = \varepsilon(1 - \varepsilon)\alpha^2.$$

Optimizing then in ε leads by (3.7) to the desired inequality $C_P(\mu_\alpha, 1) \leq 4/\alpha^2$. To get the reverse inequality, we choose in (2.3) the centered functions $f_\eta(x) = (1 + e^{-x})^\eta - 1/(\alpha - \eta)$, with $\eta < \alpha/2$ to ensure that $f_\eta \in H^1(\mu_\alpha, 1)$. After computations, it yields

$$\frac{\int_{\mathbb{R}} f_\eta^2 d\mu_\alpha}{\int_{\mathbb{R}} (f'_\eta)^2 d\mu_\alpha} = \frac{\frac{\alpha}{\alpha - 2\eta} - \frac{\alpha^2}{(\alpha - \eta)^2}}{\frac{2\alpha\eta^2}{(\alpha - 2\eta)(\alpha + 1 - 2\eta)(\alpha + 2 - 2\eta)}} = \frac{(\alpha + 1 - 2\eta)(\alpha + 2 - 2\eta)}{2(\alpha - \eta)^2},$$

and taking the limit $\eta \rightarrow \alpha/2$, we thus obtain $C_P(\mu_\alpha, 1) \geq 4/\alpha^2$.

Example 3.3. Let us concentrate now on the Pareto distribution, which is a (one-sided) heavy-tailed probability measure somewhat similar to the generalized Cauchy distribution. Given two parameters $z > 0$ and $\alpha > 0$, denote $\mu_{z,\alpha}$ the probability measure with Lebesgue density on $[z, \infty)$ defined by $x \mapsto \alpha z^\alpha/x^{\alpha+1}$. We show that $C_P(\mu_{z,\alpha}, w) = 4/\alpha^2$ when the weight is $w(x) = x^2$ (in particular it does not depend on the parameter z , as expected when using a trivial scaling argument). Hence we can assume in the sequel $z = 1$. Note that it differs from the weight emphasized in Table 1. By (3.6) we have for all $\varepsilon \in \mathbb{R}$,

$$M_{w,\varepsilon}(x) = (1 - \varepsilon) x^2 \left(\frac{\varepsilon(\alpha + 1)^2 - (\alpha + 1)}{x^2} \right), \quad x > 1.$$

To ensure the positivity of $M_{w,\varepsilon}$, we choose $\varepsilon \in (1/(\alpha + 1), 1)$. Optimizing then in ε and using (3.7) yields

$$C_P(\mu_{1,\alpha}, w) \leq \frac{4}{\alpha^2}.$$

To get the converse inequality, choose the centered functions $f_\eta(x) = x^\eta - \alpha/(\alpha - \eta)$, with $\eta < \alpha/2$ (so that they belong to $H_1(\mu_{1,\alpha}, w)$). Indeed after some computations, we get

$$\frac{\int_1^\infty f_\eta^2 d\mu_{1,\alpha}}{\int_1^\infty w (f'_\eta)^2 d\mu_{1,\alpha}} = \frac{\frac{\alpha}{\alpha - 2\eta} - \left(\frac{\alpha}{\alpha - \eta}\right)^2}{\frac{\alpha\eta^2}{\alpha - 2\eta}} = \frac{1}{(\alpha - \eta)^2},$$

and since the right-hand side converges to $4/\alpha^2$ when $\eta \rightarrow \alpha/2$, this proves the desired inequality $C_P(\mu_{1,\alpha}, w) \geq 4/\alpha^2$. Again in this situation, the weighted Poincaré inequality does admit any saturating function. Indeed, if it was the case, then there would be some smooth non-null centered function $f \in H^1(\mu_{1,\alpha}, w)$ such that

$$\begin{cases} L_w f(x) = x^2 f''(x) + (1 - \alpha)x f'(x) = -\frac{\alpha^2}{4} f(x), & x > 1, \\ f'(1) = 0. \end{cases}$$

Then one can prove that such a centered function is given by

$$f(x) = x^{\frac{\alpha}{2}} \left(1 - \frac{\alpha}{2} \log(x) \right), \quad x \geq 1,$$

but it is not an eigenfunction since $f \notin L^2(\mu_{1,\alpha})$.

Example 3.4. We consider on $(0, 1)$ the probability measure μ_α with density $\rho(x) = \alpha x^{\alpha-1}$ ($\alpha > 0$) and the asymmetric weight $w(x) = x^2(1 - x^{\alpha/2})$, $x \in [0, 1]$. Although the density might vanish at the boundary (or even be not defined at 0), it causes no trouble for the forthcoming analysis. The same remark holds for the next example. Notice that when $\alpha = 1$, μ_α stands for the uniform distribution. This time the identity (3.6) is not relevant since $\inf M_{w,\varepsilon} \leq 0$ for all $\varepsilon \in \mathbb{R}$. However we are able to prove that $C_P(\mu_\alpha, w) = 4/\alpha^2$ by using (3.4) with some convenient function h' . More precisely, since we have

$$L_w f(x) = x^2(1 - x^{\alpha/2})f''(x) + x \left(\alpha + 1 - \left(\frac{3\alpha}{2} + 1 \right) x^{\alpha/2} \right) f'(x), \quad x \in (0, 1),$$

then considering $h'(x) = x^{-\delta}$ with $\delta \in \mathbb{R}$ yields

$$M_{w,h}(x) = -(\alpha - \delta + 1)(1 - \delta) + \left(1 + \frac{\alpha}{2} - \delta \right) \left(\frac{3}{2}\alpha - \delta + 1 \right) x^{\alpha/2}, \quad x \in (0, 1),$$

which is non-negative as soon as $\delta \in [1, 1 + \alpha/2]$. Choosing then $\delta = 1 + \alpha/2$ entails by (3.5) the bound $C_P(\mu_\alpha, w) \leq 4/\alpha^2$.

To obtain the lower bound we consider the function $f_\eta(x) = x^{-\eta} - \alpha/(\alpha - \eta)$, with $\eta < \alpha/2$ (so that $f_\eta \in H^1(\mu_\alpha, w)$) and compute:

$$\frac{\int_0^1 f_\eta^2 d\mu_\alpha}{\int_0^1 w (f'_\eta)^2 d\mu_\alpha} = \frac{\frac{\alpha}{\alpha-2\eta} - \frac{\alpha^2}{(\alpha-\eta)^2}}{\frac{\alpha^2 \eta^2}{2(\alpha-2\eta)(\frac{3}{2}\alpha-2\eta)}} = \frac{3\alpha - 4\eta}{\alpha(\alpha - \eta)^2}.$$

By taking the limit $\eta \rightarrow \alpha/2$ we establish that $C_P(\mu_\alpha, w) \geq 4/\alpha^2$. Note however that an associated eigenfunction does not exist since the non-null centered function $f(x) = x^{-\alpha/2} - 2$, which solves the equation

$$L_w f(x) = -\frac{\alpha^2}{4} f(x), \quad x \in (0, 1),$$

does not belong to $L^2(\mu_\alpha)$.

Example 3.5. As a last example we consider the symmetric beta distribution on $(-1, 1)$ whose density is $\rho(x) = (1 - x^2)^{\beta-1}/Z_\beta$, where $\beta > 0$ and Z_β is the normalization constant $Z_\beta = \int_{-1}^1 (1 - x^2)^{\beta-1} dx$. Using the spectral approach, it is known that μ_β satisfies a weighted Poincaré inequality with weight $w_0(x) = 1 - x^2$ and Poincaré constant $C_P(\mu_\beta, w_0) = 1/2\beta$. In particular linear functions (through Jacobi polynomials of degree 1), are the saturating functions, see *e.g.* [2]. However we wonder if such an inequality still hold with another weight for which the spectral analysis of the underlying operator does not give immediately the expression of the Poincaré constant. Actually, we are able to prove below that a weighted Poincaré inequality holds with weight $w(x) = (1 - x^2)^2$ and corresponding Poincaré constant $C_P(\mu_\beta, w) = 1/\beta^2$ for $\beta \in (0, 1]$ (for $\beta > 1$ we obtain directly $C_P(\mu_\beta, w) = 1/(2\beta - 1)$ since the increasing centered function $x \mapsto x/\sqrt{1 - x^2} \in L^2(\mu_\beta)$ is an eigenfunction associated to the eigenvalue $2\beta - 1$ of the operator $-L_w$ below). First, as in the previous example, the identity (3.6) does not allow us to get the desired result so that let us rather use the equation (3.4) with some other convenient test function h . Since the associated operator is given for all $x \in (-1, 1)$ by

$$L_w f(x) = (1 - x^2)^2 f''(x) - 2(\beta + 1)x(1 - x^2)f'(x),$$

we obtain by plugging in (3.4) the function $h'(x) = (1 - x^2)^\delta$,

$$M_{w,h}(x) = 2(\delta + \beta + 1)(1 - (3 + 2\delta)x^2),$$

whose minimum on $[-1, 1]$ is reached at $x = \pm 1$ and positive as soon as $\delta \in (-1 - \beta, -1)$. Choosing finally $\delta = -1 - \beta/2$ implies by (3.5) the upper bound $C_P(\mu_\beta, w) \leq 1/\beta^2$.

On the other hand, we consider the function $f_\eta(x) = (1 - x^2)^\eta - Z_{\eta+\beta}/Z_\beta$ (with $\eta > -\beta/2$ to ensure $f_\eta \in H^1(\mu_\beta, w)$) and compute:

$$\frac{\int_{-1}^1 f_\eta^2 d\mu_\beta}{\int_{-1}^1 w (f'_\eta)^2 d\mu_\beta} = \frac{\frac{Z_{2\eta+\beta}}{Z_\beta} - \left(\frac{Z_{\eta+\beta}}{Z_\beta}\right)^2}{\frac{2\eta^2}{2\eta+\beta} \times \frac{Z_{2\eta+\beta+1}}{Z_\beta}}.$$

Then the continuity of $a \mapsto Z_a$ on $(0, \infty)$ together with an integration by parts leading to the following identity: for all $a > 0$,

$$Z_{a+1} = \frac{2a}{1 + 2a} Z_a,$$

entails that we finally have

$$\frac{\int_{-1}^1 f_\eta^2 d\mu_\beta}{\int_{-1}^1 w (f'_\eta)^2 d\mu_\beta} \underset{\eta \rightarrow -\beta/2}{\sim} \frac{1}{\beta^2}.$$

Hence we get the reverse inequality $C_P(\mu_\beta, w) \geq 1/\beta^2$. However for every $\beta \in (0, 1]$ there is no associated eigenfunction. Indeed, the related problem is to find some smooth non-null centered function $f \in H^1(\mu_\beta, w)$ such that

$$L_w f(x) = -\beta^2 f(x), \quad x \in (-1, 1).$$

Rewriting $f(x) = (1 - x^2)^{-\beta/2} g(x)$, this is equivalent to find some solution g such that the following Legendre equation holds: for all $x \in (-1, 1)$,

$$(1 - x^2)g''(x) - 2xg'(x) = -\beta(\beta + 1)g(x).$$

For $\beta \in (0, 1)$, solutions are linear combinations of Legendre functions of the first and second kind, the first one admitting finite limits at ± 1 whereas the second one, denoted Q_β , is singular at the endpoints ± 1 , see [24]. In particular we have the asymptotics $Q_\beta(x) \underset{x \rightarrow 1}{\sim} -\log(1 - x)/2$ so that the resulting function $f(x) = (1 - x^2)^{-\beta/2} g(x)$ does not belong to $L^2(\mu_\beta)$. Finally for $\beta = 1$, solutions to the Legendre equation are linear (*i.e.*, degree 1 Legendre polynomials) but also in this case we have $f \notin L^2(\mu_\beta)$.

To conclude, let us prove that for every $\beta > 0$, the exponent 2 in $w(x) = (1 - x^2)^2$ is the largest one leading to a weighted Poincaré inequality. Suppose by contradiction that there exists some $\varepsilon > 0$ such that $w_\varepsilon(x) = (1 - x^2)^{2+\varepsilon}$ is an admissible weight. By (2.3) applied to the function $f_\eta(x) = (1 - x^2)^\eta - Z_{\eta+\beta}/Z_\beta$, $\eta > -\beta/2$, it follows that

$$C_P(\mu, w_\varepsilon) \geq \frac{Z_{2\eta+\beta} - \frac{Z_{\eta+\beta}^2}{Z_\beta}}{4\eta^2 (Z_{2\eta+\beta+\varepsilon} - Z_{2\eta+\beta+\varepsilon+1})},$$

which tends to infinity for each fixed $\varepsilon > 0$ as $\eta \rightarrow -\beta/2$, leading thus to a contradiction.

4. LINK WITH GLOBAL SENSITIVITY ANALYSIS

Let us turn our attention to the consequences of weighted Poincaré inequalities for sensitivity analysis. First we provide the proof of the inequality involving total Sobol and weighted DGSM indices defined earlier in the introduction. Subsequently we deal with the equality case and emphasize a stability condition ensuring the sharpness of the upper bounds and introduce data-driven weights, together with a uniform consistency result. At the end, we address the Poincaré chaos approach to produce lower bounds for total Sobol indices.

In the whole section, we consider a random vector $X = (X_1, \dots, X_d) \in \mathbb{R}^d$ of independent input variables and the output $f(X) \in L^2$, where $f: \mathbb{R}^d \rightarrow \mathbb{R}$ is some function referring to the model. Recall that for a set $I \subset \{1, \dots, d\}$ the notation X_I stands for the random vector defined by the variables X_j , $j \in I$. As defined in the introduction, the total Sobol indices are given by

$$S_i^{\text{tot}}(f(X)) = \frac{\text{Var}(f_i^{\text{tot}}(X))}{\text{Var}(f(X))},$$

where

$$f_i^{\text{tot}}(X) = \sum_{I \ni i} f_I(X_I) = f(X) - \mathbb{E}[f(X) | X_{-i}], \quad (4.1)$$

the random vector X_{-i} of dimension $d - 1$ being defined by $X_{-i} := X_{\{1, \dots, d\} \setminus \{i\}}$. Note that the second equality in (4.1), which is important in the forthcoming analysis, comes from the fact that if I is a superset of $\{i\}$, then by the assumptions of the Sobol-Hoeffding decomposition,

$$\mathbb{E}[f_I(X_I) | X_{-i}] = \mathbb{E}[f_I(X_I) | X_{I \setminus \{i\}}] = 0.$$

Finally, given $i \in \{1, \dots, d\}$ and some convenient non-negative weight w_i , we further assume that $(w_i(X_i))^{1/2} \frac{\partial f}{\partial x_i}(X) \in L^2$. Then, the weighted DGSM index related to the distribution of the input X_i is defined as

$$\nu_{i, w_i}(f(X)) = \mathbb{E} \left[w_i(X_i) \left(\frac{\partial f}{\partial x_i}(X) \right)^2 \right].$$

To simplify the notation, we write S_i^{tot} for $S_i^{\text{tot}}(f(X))$ and ν_{i, w_i} for $\nu_{i, w_i}(f(X))$.

4.1. Upper bounds for total Sobol indices

The following proposition deals with the inequality announced in the introduction, linking total Sobol and weighted DGSM indices. It generalizes the result presented in [19] for classical Poincaré inequalities.

Proposition 4.1. *Given $i \in \{1, \dots, d\}$, assume that the distribution μ_i of the input variable X_i belongs to $\mathcal{P}(a_i, b_i)$. Let $w_i \in \mathcal{W}(a_i, b_i)$ be a weight function and suppose that μ_i satisfies the following weighted Poincaré inequality: for all centered function $g \in H^1(\mu_i, w_i)$,*

$$\mathbb{E}[g(X_i)^2] \leq C_P(\mu_i, w_i) \mathbb{E}[w_i(X_i)g'(X_i)^2]. \quad (4.2)$$

We also assume that $(w_i(X_i))^{1/2} \frac{\partial f}{\partial x_i}(X) \in L^2$ where $f(X) \in L^2$. Then,

$$S_i^{\text{tot}} \leq C_P(\mu_i, w_i) \frac{\nu_{i, w_i}}{\text{Var}(f(X))}. \quad (4.3)$$

Proof. For all $x_{-i} \in \prod_{j \neq i} [a_j, b_j]$, let $g_{x_{-i}}$ be the one-dimensional function

$$g_{x_{-i}} : x_i \in [a_i, b_i] \mapsto f_i^{\text{tot}}(x).$$

Notice that, from (4.1), we can write $g_{x_{-i}}(x_i) = f(x) - \mathbb{E}[f(X) | X_{-i} = x_{-i}]$. Under this form, it is clear that $g_{x_{-i}}$ is a centered function of $L^2(\mu_i)$ and verifies

$$g'_{x_{-i}}(x_i) = \frac{\partial f}{\partial x_i}(x).$$

Under the assumptions on f , this latter equality shows that $g_{x_{-i}}$ belongs to $H^1(\mu_i, w_i)$. Then the weighted Poincaré inequality (4.2) applied to $g_{x_{-i}}$ gives

$$\mathbb{E} \left(f_i^{\text{tot}}(X)^2 | X_{-i} = x_{-i} \right) \leq C_P(\mu_i, w_i) \mathbb{E} \left[w_i(X_i) \left(\frac{\partial f}{\partial x_i}(X) \right)^2 \Big| X_{-i} = x_{-i} \right].$$

Integrating over x_{-i} with respect to the product measure $\otimes_{j \neq i} \mu_j$ and using the fact that f_i^{tot} is centered, we get

$$\text{Var} \left(f_i^{\text{tot}}(X) \right) \leq C_P(\mu_i, w_i) \mathbb{E} \left[w_i(X_i) \left(\frac{\partial f}{\partial x_i}(X) \right)^2 \right].$$

Dividing by $\text{Var}(f(X))$ concludes the proof. \square

4.2. Case of equality in the upper bound and stability

Looking carefully at the proof of Proposition 4.1 above, we observe that a sufficient condition ensuring the equality in (4.3) is that the one-dimensional function $x_i \mapsto f_i^{\text{tot}}(x)$ saturates the weighted Poincaré inequality (4.2) for each fixed $x_{-i} \in \mathbb{R}^{d-1}$. Since the space of saturating functions is one-dimensional (it corresponds to the eigenspace related to the spectral gap of the underlying diffusion operator), the function f_i^{tot} is then required to be of the following form:

$$f_i^{\text{tot}}(x) = g_i(x_i)v(x_{-i}), \quad x \in \mathbb{R}^d,$$

where $g_i \in H^1(\mu_i, w_i)$ is some one-dimensional function saturating the weighted Poincaré inequality (4.2) (in particular it is centered with respect to μ_i) and v_i is a function that only depends on x_{-i} . In this case the function f rewrites as

$$f(x) = u_i(x_{-i}) + g_i(x_i)v_i(x_{-i}), \quad x \in \mathbb{R}^d,$$

with $u_i(x_{-i}) = \mathbb{E}[f(X) | X_{-i} = x_{-i}]$. The next proposition further provides a stronger result in terms of stability of the inequality (4.3), at least when the one-dimensional function considered is close to the function saturating the Poincaré inequality (4.2) in the space $H^1(\mu_i, w_i)$ (it corresponds below to the case $\varepsilon > 0$).

Proposition 4.2. *Under the notation and assumptions of Proposition 4.1, let fix $i \in \{1, \dots, d\}$ and let f be of the form $f(x) = u_i(x_{-i}) + h_i(x_i)v_i(x_{-i})$, where u_i, v_i are functions depending only on x_{-i} , such that $u_i(X_{-i}), v_i(X_{-i}) \in L^2$, and $h_i \in H^1(\mu_i, w_i)$ is centered with respect to μ_i . Let further assume that there exists $\varepsilon \geq 0$ such that*

$$\mathbb{E} \left[w_i(X_i) (h'_i(X_i) - g'_i(X_i))^2 \right] \leq \varepsilon,$$

where g_i is a function saturating the weighted Poincaré inequality (4.2). Then we have the following stability result:

$$0 \leq C_P(\mu_i, w_i) \frac{\nu_{i, w_i}}{\text{Var}(f(X))} - S_i^{\text{tot}} \leq C_P(\mu_i, w_i) \frac{\mathbb{E} [v_i^2(X_{-i})]}{\text{Var}(f(X))} \varepsilon.$$

In particular, if f has the form $f(x) = u_i(x_{-i}) + g_i(x_i)v_i(x_{-i})$, then (4.3) is an equality.

Proof. Denote V the symmetric bilinear form acting on the space of centered functions in $H^1(\mu_i, w_i)$ as follows:

$$V(\varphi, \psi) = C_P(\mu_i, w_i) \mathbb{E}[w_i(X_i) \varphi'(X_i) \psi'(X_i)] - \mathbb{E}[\varphi(X_i) \psi(X_i)].$$

By the weighted Poincaré inequality (4.2), the induced quadratic form is non-negative. Moreover we have

$$V(h_i - g_i, h_i - g_i) = V(h_i, h_i) + V(g_i, g_i) - 2V(h_i, g_i).$$

Since the function g_i saturates (4.2), we have $V(g_i, g_i) = 0$ and also $V(h_i, g_i) = 0$, using the variational identity (2.4). Hence we get

$$0 \leq V(h_i, h_i) = V(h_i - g_i, h_i - g_i) \leq C_P(\mu_i, w_i) \varepsilon. \quad (4.4)$$

Notice that $\frac{\partial f}{\partial x_i}(x) = h'_i(x_i) v_i(x_{-i})$ and $f_i^{\text{tot}}(x) = h_i(x_i) v_i(x_{-i})$. Then, by independence of X_i and X_{-i} , we obtain:

$$C_P(\mu_i, w_i) \frac{\nu_{i, w_i}}{\text{Var}(f(X))} - S_i^{\text{tot}} = \frac{\mathbb{E}[v_i^2(X_{-i})]}{\text{Var}(f(X))} V(h_i, h_i).$$

Combining with (4.4) concludes the proof. \square

Although w_i can be any general weight in $\mathcal{W}(a_i, b_i)$ *a priori*, the requirement that the function g_i saturates the weighted Poincaré inequality (4.2) enforces w_i to be proportional to the weight w_{g_i} constructed according to Theorem 3.1. Indeed, it is not difficult to prove that necessarily $w_i = w_{g_i}/C_P(\mu_i, w_i)$.

4.3. Data-driven weights for monotonic main effects

Important quantities arising in GSA are the first-order indices, or main effects, which allow to understand the influence of each variable individually over the model. For each $i \in \{1, \dots, d\}$, the main effect $f_i(X_i)$ (or simply f_i , using a slight abuse of language) of the input variable X_i is defined as

$$f_i(X_i) = \mathbb{E}[f(X) | X_i] - \mathbb{E}[f(X)].$$

By definition of the conditional expectation, $f_i(X_i)$ is the best centered L^2 approximation of $f(X)$ by a one-dimensional function depending on X_i . It is thus reasonable to use f_i for building w_i . If f_i belongs to $\mathcal{C}_*^{1,2}(a_i, b_i)$, implying that f_i is strictly monotonic, a natural candidate for w_i is w_{f_i} since by Theorem 3.1, f_i saturates the corresponding weighted Poincaré inequality. By Proposition 4.2, this further implies that the total Sobol indices will be perfectly approximated by weighted DGSM ones involving the weight w_{f_i} for functions of the form $f(x) = u_i(x_{-i}) + h_i(x_i)v_i(x_{-i})$. Indeed, then we necessarily have $f_i(x_i) = h_i(x_i) \mathbb{E}[v_i(X_{-i})]$, and (provided that $\mathbb{E}[v_i(X_{-i})] \neq 0$) h_i is proportional to f_i , corresponding to an equality case in Proposition 4.1.

In practice, however, f_i is unknown and must be estimated. The idea is to use some convenient pointwise estimator \widehat{w}_i of w_{f_i} , *i.e.*, $\widehat{w}_i(x_i)$ is an estimator of $w_{f_i}(x_i)$ for all $x_i \in [a_i, b_i]$. A natural candidate for this data-driven weight \widehat{w}_i is obtained by first approximating f_i with a pointwise strictly monotonic estimator \widehat{f}_i , almost surely centered with respect to μ_i , and then considering $\widehat{w}_i = w_{\widehat{f}_i}$. The consistency of this statistical procedure is proved in the following proposition.

Proposition 4.3. *Given $i \in \{1, \dots, d\}$ and a finite interval $[a_i, b_i]$, we assume that $\mu_i \in \mathcal{P}(a_i, b_i)$ and that the main effect $f_i \in \mathcal{C}_*^{1,2}(a_i, b_i)$ satisfies $f_i'(a) \neq 0$ and $f_i'(b) \neq 0$. Moreover we assume that $\frac{\partial f}{\partial x_i}(X) \in L^2$.*

Let $(X_1, \dots, X^{(n)})$ be an i.i.d. sample generated from X and consider an estimator \widehat{f}_i constructed with respect to this sample. We assume the following (almost sure) hypothesis:

- (i) \widehat{f}_i is centered with respect to μ_i .
- (ii) $\widehat{f}_i \in \mathcal{C}_*^{1,2}(a_i, b_i)$ satisfies $\widehat{f}_i'(a) \neq 0$ and $\widehat{f}_i'(b) \neq 0$.
- (iii) \widehat{f}_i converges uniformly to f_i on $[a_i, b_i]$ as $n \rightarrow \infty$.
- (iv) \widehat{f}_i' converges uniformly to f_i' on $[a_i, b_i]$ as $n \rightarrow \infty$.

Then almost surely, the data-driven weight $\widehat{w}_i = w_{\widehat{f}_i}$ converges uniformly to w_{f_i} on $[a_i, b_i]$ as $n \rightarrow \infty$. Moreover, the Monte-Carlo estimator

$$\widehat{\nu}_i = \frac{1}{n} \sum_{k=1}^n \widehat{w}_i(X_i^{(k)}) \left| \frac{\partial f}{\partial x_i}(X^{(k)}) \right|^2$$

converges almost surely to $\nu_{i, w_{f_i}}$ as $n \rightarrow \infty$.

Proof. Using (i) and (ii), the weight $\widehat{w}_i = w_{\widehat{f}_i}$ is defined in Theorem 3.1 for all $x_i \in [a_i, b_i]$ by

$$\widehat{w}_i(x_i) = -\frac{1}{\widehat{f}_i'(x_i)\rho_i(x_i)} \int_{a_i}^{x_i} \widehat{f}_i(y)\rho_i(y) dy. \quad (4.5)$$

Since a.s. \widehat{f}_i converges uniformly to f_i on $[a_i, b_i]$ as $n \rightarrow \infty$, it follows that a.s. the sequence $x_i \mapsto \int_{a_i}^{x_i} \widehat{f}_i(y)\rho_i(y) dy$ also converges uniformly to $x_i \mapsto \int_{a_i}^{x_i} f_i(y)\rho_i(y) dy$ on $[a_i, b_i]$. By (ii), \widehat{f}_i and f_i are \mathcal{C}^1 on the finite interval $[a_i, b_i]$. Since \widehat{f}_i' tends uniformly to f_i' and \widehat{f}_i' is of constant sign, the function $|\widehat{f}_i'|$ is bounded from below by a positive constant that does not depend on n . The same argument holds for $|f_i'|$ as well. Using that ρ_i is also bounded from below by some positive constant, this further implies that $1/(\widehat{f}_i'\rho_i)$ converges uniformly to $1/(f_i'\rho_i)$ on $[a_i, b_i]$. This concludes the proof of the desired a.s. uniform convergence of \widehat{w}_i .

Now the proof of the convergence of the Monte-Carlo estimator $\widehat{\nu}_i$ to the weighted DGSM index $\nu_{i, w_{f_i}}$ is straightforward: decomposing $\widehat{\nu}_i$ as

$$\widehat{\nu}_i = \frac{1}{n} \sum_{k=1}^n \left(\widehat{w}_i(X_i^{(k)}) - w_{f_i}(X_i^{(k)}) \right) \left| \frac{\partial f}{\partial x_i}(X^{(k)}) \right|^2 + \frac{1}{n} \sum_{k=1}^n w_{f_i}(X_i^{(k)}) \left| \frac{\partial f}{\partial x_i}(X^{(k)}) \right|^2,$$

we observe on the first hand that the first term converge a.s. to 0 (since a.s. \widehat{w}_i converges uniformly to w_{f_i} on $[a_i, b_i]$ as $n \rightarrow \infty$ and $\frac{\partial f}{\partial x_i}(X) \in L^2$) whereas on the other hand the second term converges a.s. to $\nu_{i, w_{f_i}}$ by the strong law of large numbers. The proof is now complete. \square

Note that the assumptions of Proposition 4.3 are rather strong. A difficulty is to ensure that \widehat{f}_i' can be bounded from below by a positive constant that does not depend on the sample size n . This is guaranteed by the uniform convergence of the derivatives \widehat{f}_i' . Notice also that Assumption (iii) may be replaced by

- (iii') there exists some $c_i \in [a_i, b_i]$ such that $\widehat{f}_i(c_i)$ converges to $f_i(c_i)$ as $n \rightarrow \infty$

since (iii') and (iv) imply (iii). This is however a particular case, and we have chosen to keep here the most general assumption.

Note also that the relevance of the data-driven weight methodology depends crucially on the construction of the strictly monotonic \widehat{f}_i which estimates the main effect f_i . In practice it is difficult to provide such a construction ensuring the monotonicity and the uniform consistency properties at the same time. See however the paper [23] which explains how to modify a given uniformly consistent estimator to obtain a monotonic version of it. In particular the uniform consistency property is preserved with the same rate of convergence.

To achieve the discussion about data-driven weights, we point out that the previous approach can not be applied in theory when the main effect f_i is not monotonic. Indeed, the weight w_{f_i} is not well defined and the required convergence properties of the estimator \widehat{f}_i are not guaranteed. However in practice such a procedure can be adapted when the strictly monotonic estimator \widehat{f}_i remains close to f_i (in the weighted Sobolev space related to \widehat{w}_i), so that the numerical results obtained with the data-driven weight \widehat{w}_i may be somewhat relevant in this context.

4.4. Approximations of total Sobol indices with Poincaré chaos expansions

In the previous sections, our main objective was to bound from above the total Sobol indices with the weighted DGSM ones. However when we consider a weight w_i that does not vanish on the finite interval $[a_i, b_i]$, the associated Sturm-Liouville problem is regular and the underlying diffusion operator $L_{w_i}g = (w_i g' \rho_i)' / \rho_i$ admits a discrete spectral decomposition. Collecting all these decompositions for all $i \in \{1, \dots, d\}$, such a decomposition considered on the product space leads to the so-called Poincaré chaos expansion and allows us to expand $\text{Var}(f_i^{\text{tot}}(X))$. As such, truncating the expansion yields to lower bounds on the total Sobol index S_i^{tot} . Below we provide further details on this approach involving weights, which is a simple adaptation of the one presented in [21, 27] and related to classical Poincaré inequalities.

Before stating our desired expansion, we need to fix some elements. For each $i \in \{1, \dots, d\}$, recall that each $\mu_i \in \mathcal{P}(a_i, b_i)$ stands for the distribution of the input variable X_i . Let $w_i \in \mathcal{W}(a_i, b_i)$ which does not vanish at the boundaries. Denote $(\lambda_{i,n})_{n \in \mathbb{N}}$ the eigenvalues listed in increasing order of the diffusion operator $-L_{w_i}$. We have $\lambda_{i,0} = 0$ and $\lambda_{i,1} = 1/C_P(\mu_i, w_i)$ is the spectral gap. Let $(e_{i,n})_{n \in \mathbb{N}}$ be the associated orthonormal basis of eigenfunctions (recall that $e_{i,0} \equiv 1$), the normalization being understood in $L^2(\mu_i)$.

In higher dimension we consider the product measure $\mu = \mu_1 \otimes \dots \otimes \mu_d$ of the input vector X . Letting $L^2(\mu)$ be the space of square-integrable functions on the cartesian product $\prod_{i=1}^d [a_i, b_i]$ with respect to μ , we write the scalar product of two given functions $\varphi, \psi \in L^2(\mu)$ as $\langle \varphi, \psi \rangle = \int \varphi \psi d\mu$. Then the diffusion operator related to μ is the sum of the one-dimensional operators $-L_{w_i}$, each acting only on the i -th coordinate of a given multi-dimensional function, the other coordinates being fixed. Then the collection of all tensor-product functions $e_\alpha : x \mapsto \prod_{i=1}^d e_{i,\alpha_i}(x_i)$, with $\alpha = (\alpha_1, \dots, \alpha_d) \in \mathbb{N}^d$ a multi-index, form an orthonormal basis of $L^2(\mu)$ and correspond to the eigenfunctions of this multi-dimensional diffusion operator, each eigenfunction e_α being related to the eigenvalue $\sum_{i=1}^d \lambda_{i,\alpha_i}$. Hence every function in $L^2(\mu)$ admits a decomposition in terms of the functions $(e_\alpha)_{\alpha \in \mathbb{N}^d}$, known as the

Poincaré chaos expansion (PoinCE). Applied to the function f , we have

$$f = \sum_{\alpha \in \mathbb{N}^d} \langle f, e_\alpha \rangle e_\alpha.$$

Since we have for all $x \in \prod_{i=1}^d [a_i, b_i]$,

$$f_i^{\text{tot}}(x) = f(x) - \int_{a_i}^{b_i} f(x_1, \dots, x_i, \dots, x_d) \mu_i(dx_i),$$

its PoinCE has the particular form

$$f_i^{\text{tot}} = \sum_{\substack{\alpha \in \mathbb{N}^d \\ \alpha_i \geq 1}} \langle f, e_\alpha \rangle e_\alpha.$$

Hence the variance of the random variable $f_i^{\text{tot}}(X)$ can be expanded using Parseval's identity:

$$\text{Var}(f_i^{\text{tot}}(X)) = \sum_{\substack{\alpha \in \mathbb{N}^d \\ \alpha_i \geq 1}} \langle f, e_\alpha \rangle^2. \quad (4.6)$$

The advantage of using such a basis $(e_\alpha)_{\alpha \in \mathbb{N}^d}$ rather than any other one resides in the fact that it provides an alternative expansion in terms of the derivatives of f , in the spirit of the one-dimensional identity (2.4): for all $i \in \{1, \dots, d\}$ and all $n \in \mathbb{N}$,

$$\langle f, e_{i,n} \rangle = \frac{1}{\lambda_{i,n}} \langle w_i \frac{\partial f}{\partial x_i}, e'_{i,n} \rangle.$$

The next proposition summarizes these facts. The proof is somewhat similar to the one established in [27].

Proposition 4.4. *Assume that the weighted DGSM index ν_{i,w_i} is finite. Then the Parseval's identity (4.6) can be rewritten using derivatives as:*

$$\text{Var}(f_i^{\text{tot}}(X)) = \sum_{\substack{\alpha \in \mathbb{N}^d \\ \alpha_i \geq 1}} \frac{1}{\lambda_{i,\alpha_i}^2} \langle w_i \frac{\partial f}{\partial x_i}, e'_{i,\alpha_i} \prod_{j \neq i} e_{j,\alpha_j} \rangle^2. \quad (4.7)$$

In practice, the decompositions (4.6) and (4.7) have to be appropriately truncated, leading to approximations of the Sobol index S_i^{tot} . Thus, the key point is how to choose the truncation and then to estimate the various scalar products. Certainly, keeping only few terms in the Poincaré chaos expansion might provide relevant numerical results, as we will observe in Section 5 when dealing with our toy models and the real flood application. However it is not an easy task in full generality as soon as the dimension is large since the computational cost is high. A first step in this direction has been proposed in [21] in the context of classical Poincaré inequalities using sparse regression. In particular this approach allows to compute simultaneously the scalar products involved in the decompositions (4.6) and (4.7). Dealing with the weighted case, we intend to apply the same methodology in a future work.

As a last remark, we mention that the data-driven approach emphasized in Section 4.3 is hardly available at this stage when using the Poincaré chaos expansion, since in the latter case the data-driven weight \widehat{w}_i is required to be positive on $[a_i, b_i]$. In other words, it means that the derivatives of the estimator \widehat{f}_i should vanish at the boundary, a property which is hard to guarantee in practice.

4.5. Summary and guidelines for choosing weights to GSA

Before turning to Section 5 and the applications to various models arising in GSA, let us for completeness summarize our approach based on weighted Poincaré inequalities. Recall that for a given $i \in \{1, \dots, d\}$ the total Sobol indices S_i^{tot} can be bounded from above by an expression involving the weighted DGSM index ν_{i,w_i} with an appropriate weight w_i (see Section 4.1). Lower bounds on S_i^{tot} are also available when using the Poincaré chaos expansion, as emphasized in the last section. To do so, we study the spectral properties of the diffusion operator $L_{w_i}g = (w_i g' \rho_i)' / \rho_i$ depending on the weight w_i which has to be constructed conveniently.

When no particular knowledge about the model f is provided, the most information we can expect may be given by the one-dimensional L^2 centered approximation of $f(X)$ corresponding to the main effect $f_i(X_i)$ in the Sobol Hoeffding decomposition. Then we can tune the (one-dimensional) weight w_i such that the first non-null eigenfunction e_i of the operator $-L_{w_i}$ (constructed with respect to w_i) is close to f_i . Notice however that this approximation is constrained by the structural properties of e_i , in particular its monotonicity.

In many engineering problems, f_i may be approximated by a linear function. This justifies the idea of choosing w_{lin} (see Section 3.2) by default or its Gaussian approximation w_{G} (see Section 3.3). Nevertheless, as a first step of GSA, it is often possible to visualize the main effects and to estimate them from a sample of small size, see for instance [18]. Thus it is natural to consider the data-driven weight \widehat{w}_i built from a strictly monotonic estimator \widehat{f}_i of f_i (see Section 4.3). As mentioned earlier, we illustrate this data-driven approach only for bounding from above the total Sobol indices, as their estimation from Poincaré chaos expansions requires that the derivatives of the estimator \widehat{f}_i vanishes at the boundary, a property which is difficult to ensure in practice. A first idea in this direction could be to use a Gaussian process approach for constraints on boundedness, monotonicity and convexity, cf. e.g. [20].

5. APPLICATIONS

5.1. Numerical settings

In this final part, we present numerical applications of our results on two toy models and a more realistic one given by a flood case. To emphasize the role of the input variables X_i , $i \in \{1, \dots, d\}$, we rewrite the weights presented in Section 3 as $w_{i,\text{lin}}$, $w_{i,\text{G}}$ and $w_{i,\text{U}}$. In addition to $w_{i,\text{lin}}$ and \widehat{w}_i , we consider also the non-vanishing weights $w_{i,\text{U}}$ and $w_{i,\text{G}}$ (see Section 3.3) for comparison purposes when bounding from above total Sobol indices. For the lower bounds using Poincaré chaos expansion (understood in this part as approximations), we employ only the weights $w_{i,\text{G}}$ and $w_{i,\text{U}}$, which ensure the existence of an orthonormal basis of eigenfunctions. We refer to truncations of the infinite sum in (4.6) as derivative-free approximations (abbreviated Der-free) and to truncations of the one in (4.7) as derivative-based approximations (abbreviated Der-based). All our numerical results have been done with the R software [28], and are compared with the ones obtained in the classical unweighted case. We now give more specific details.

Eigenvalue and eigenfunction estimation, and PoinCE series truncation

The eigenvalues and eigenfunctions are computed using a weighted adaptation of the function `PoincareOptimal` from the package `sensitivity` [17], based on a finite element discretization. Once this is done, the PoinCE approximations can be

computed. We approximate each S_i^{tot} with truncations of both sums (4.6) and (4.7) by considering only few terms, according to the following subset of multi-indices:

$$\mathcal{A}_i = \left\{ \alpha \in \mathbb{N}^d \mid \alpha_i \in \{1, 2\}, \sum_{j \neq i} \alpha_j \leq 1 \right\}.$$

In other words, a given $\alpha \in \mathcal{A}_i$ if and only if $\alpha_i \in \{1, 2\}$ and there is at most one index $j \neq i$ such that $\alpha_j \leq 1$, all the other ones being null. As we will observe below, this selection is sufficient to obtain relevant results on the three models.

Weight computation

Recall that in our approach, given $i \in \{1, \dots, d\}$, a weight w_i is constructed from a strictly monotonic function g which saturates the associated weighted Poincaré inequality. For $w_{i,\text{lin}}$ and $w_{i,\text{U}}$, the function g is explicit. For $w_{i,\text{G}}$, as g saturates a classical (unweighted) Poincaré inequality, we compute it with the function `PoincareOptimal`, using a sequence of 500 equally spaced nodes. For \widehat{w}_i , we choose g as the monotonic estimator \widehat{f}_i of f_i given by the Shape Constrained Additive Model (SCAM) [25] from a sample of size 150. Finally, given g , the weights $w_{i,\text{lin}}$, $w_{i,\text{G}}$, $w_{i,\text{U}}$ and \widehat{w}_i are approximated with the numerical method described in Section 3.4, using a sequence of 500 equally spaced nodes.

Monte-Carlo estimation and sample size

Monte-Carlo integration is employed for computing the variance, weighted DGSM, and PoinCE scalar products, using a sample of input vectors and their corresponding outputs. When the derivatives of the outputs are unknown, we estimate them using finite differences. We have used a reasonably small sample size of 150 for the three models considered, whose dimensions are 5 for the two first ones, and 8 for the flood model. Additionally, due to estimation error in Monte-Carlo simulations, we have also used a larger sample of size 10 000 when computing the PoinCE approximations, in order to highlight the benefits of incorporating weights. Furthermore, we perform 100 bootstrap replicates for each estimation of the upper bounds and approximations. They are displayed with boxplots to represent confidence intervals.

5.2. Illustration with toy models

The two toy models we consider in this part depend on $X = (X_1, \dots, X_5)$, a vector of i.i.d. random variables with common distribution μ_i being uniform on $(0, 1)$. As such, for each $i \in \{1, \dots, d\}$, the weight $w_{i,\text{U}}$ takes the constant value $w_{i,\text{U}} \equiv C_P(\mu_i, 1) = 1/\pi^2$ and thus their upper bounds and PoinCE approximations match with the classical ones. We exclude $w_{i,\text{U}}$ in the presentation of our results below.

A simple polynomial toy model

As a first toy model we propose

$$f(X) = X_1 + X_2^2 + X_3^3 + X_4^4 + X_5^5. \quad (5.1)$$

Then for every $i \in \{1, \dots, d\}$, the function f_i^{tot} coincides with the main effect f_i and we have

$$f_i^{\text{tot}}(X_i) = f_i(X_i) = X_i^i - \frac{1}{1+i}.$$

Then the theoretical Sobol index in this case is

$$S_i^{\text{tot}} = \frac{\frac{1}{2i+1} - \frac{1}{(1+i)^2}}{\sum_{j=1}^5 \left(\frac{1}{2j+1} - \frac{1}{(1+j)^2} \right)}.$$

Figure 5 displays the upper bounds for total Sobol indices. We can see that for each input variable X_i , the data-driven weight \widehat{w}_i gives the most accurate result. This is expected because our toy function is a model with separated variables and has monotonic main effects. Indeed, from Proposition 4.2, the optimal weight is w_{f_i} , and the upper bound equals the total Sobol index. Furthermore, the estimation of the main effects is here very accurate, as shown in Figure 6. Note additionally that the classical (unweighted) upper bounds provides the worst result.

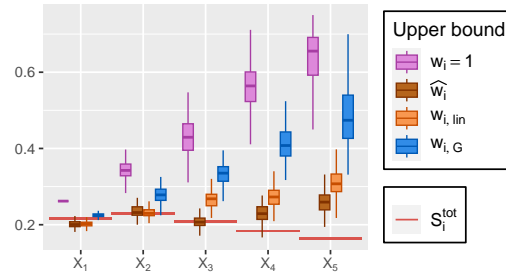


FIGURE 5. Upper bounds on the total Sobol indices for the toy model (5.1). Horizontal red bars indicate the true values.

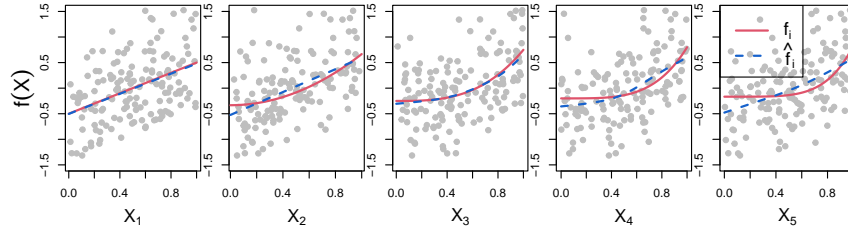


FIGURE 6. Monotonic estimators \widehat{f}_i of the main effects f_i for the toy model (5.1). In this figure, the output has been recentered.

Next, Figure 7 presents the PoinCE approximations of each total Sobol index. The estimations using a large sample size indicate that, for each X_i , the weight $w_{i,G}$ produces the most accurate approximations when comparing with the classical (unweighted) case. Finally, note that the derivative-based approximations exhibit considerably less variance than the derivative-free ones. This is because the derivatives of the function f have less fluctuations than the function itself.

A toy model separating variables, with monotonic main effects.

Let us propose a second toy model admitting interactions between input variables. Such a model, which might be useful to create toy examples to test the relevance

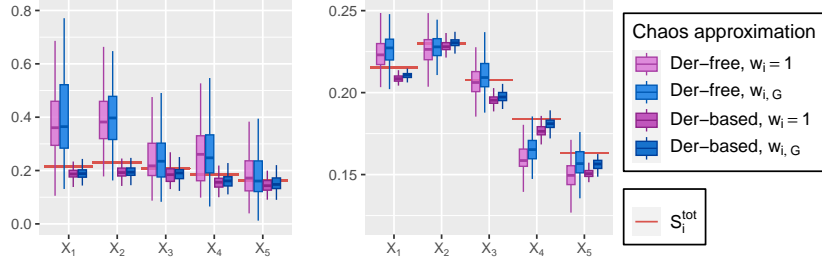


FIGURE 7. PoinCE approximations of the total Sobol indices for the toy model (5.1), estimated with samples of size 150 (left) and 10 000 (right). Horizontal red bars indicate the true values.

of GSA methodologies, is of the following form:

$$f(X) = \prod_{i=1}^d \left(\frac{h_i(X_i)}{1 + a_i} + 1 \right), \quad (5.2)$$

where $X = (X_1, \dots, X_d)$ is a vector of independent random variables, $a \in \mathbb{R}^d$ is a constant vector with non-negative coordinates and each h_i is a one-dimensional function such that $\mathbb{E}[h_i(X_i)] = 0$. Such formulation is inspired by the g -Sobol function, classical in GSA, defined with the particular choice $h_i(x_i) = 4|x_i - 1/2| - 1$. Actually, it is clear that the main effect of each input variable X_i is $f_i(X_i) = h_i(X_i)/(1 + a_i)$, so that a_i determines its main influence. Moreover, a_i determines the total influence as well. Indeed, since

$$f_i^{\text{tot}}(X) = \frac{h_i(X_i)}{1 + a_i} \prod_{j \neq i} \left(1 + \frac{h_j(X_j)}{1 + a_j} \right),$$

we thus obtain after some brief computations,

$$\text{Var}(f_i^{\text{tot}}(X)) = \frac{r_i}{(1 + a_i)^2} \prod_{j \neq i} \left(1 + \frac{r_j}{(1 + a_j)^2} \right),$$

and

$$\text{Var}(f(X)) = \prod_{j=1}^d \left(1 + \frac{r_j}{(1 + a_j)^2} \right) - 1,$$

where $r_i = \mathbb{E}[h_i(X_i)^2]$, and one deduces that the total Sobol index S_i^{tot} is small as a_i is large.

We now consider a particular case of (5.2) by choosing $h_i(x_i) = x_i^4 - \frac{1}{5}$ ($i = 1, \dots, 5$) and $a = (1, 2, 4.5, 90, 90)$. In particular, each main effect f_i is monotonic. Figure 8 presents the upper bounds. Once again, for each variable X_i , the most efficient weight is \widehat{w}_i . This illustrates the advantage of the data-driven approach with models presenting interactions between variables. Note also that for the input variable X_1 , it provides the unique relevant upper bound (the classical upper bound in the unweighted case $w_i = 1$ and the one using $w_{i,G}$ with $i = 1$ do not appear in the figure as they are greater than one). The precision of these upper bounds is explained by the accuracy of each estimator \widehat{f}_i , as we can see in Figure 9. Concerning the PoinCE approximations, the best estimations are once again the ones provided by the weight $w_{i,G}$ (see Figure 10).

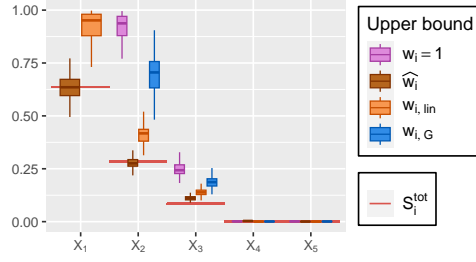


FIGURE 8. Upper bounds on the total Sobol indices for the toy model (5.2). Horizontal red bars indicate the true values.

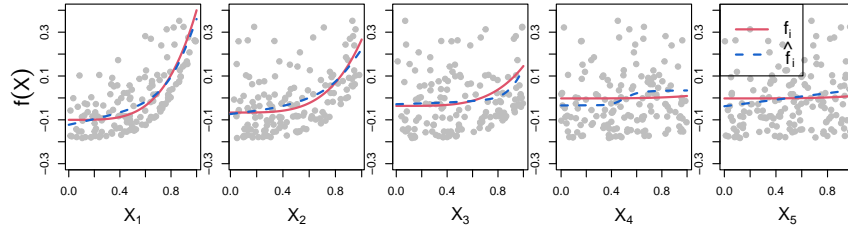


FIGURE 9. Monotonic estimators \hat{f}_i of the main effects f_i for the toy model (5.2). In this figure, the output has been recentered.

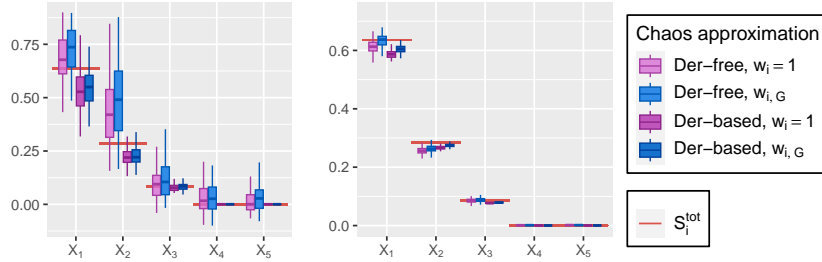


FIGURE 10. PoinCE approximations, estimated with samples of sizes 150 (left) and 10 000 (right), of the total Sobol indices for the toy model (5.2). Horizontal red bars indicate the true values.

5.3. Application to a flood model

To finish this work, we consider a simplified flood model commonly used to test GSA methodologies. It has been addressed, for instance, in [16, 21, 26, 27]. The outputs of interest are:

- the maximal annual overflow (measured in meters)

$$S = Z_v - H_d - C_b + \left(\frac{Q}{BK_s} \sqrt{\frac{L}{Z_m - Z_v}} \right)^{\text{exp3}}.$$

- the annual cost of the dyke maintenance in million of euros

$$C = \mathbb{1}_{S>0} + \left(0.2 + 0.8 \left(1 - e^{-\frac{1000}{S^4}} \right) \right) \mathbb{1}_{S \leq 0} + \frac{1}{20} \max \{H_d, 8\}.$$

The inputs are supposed to be independent random variables, whose distributions are in accordance with the empirical distributions obtained from measurement campaigns. Details are given in Table 2.

Input	Meaning	Unit	Probability measure
$X_1 = Q$	Max. flow rate	m^3/s	Gumbel $\mathcal{G}(1013, 558) _{[500, 3000]}$
$X_2 = K_s$	Strickler coefficient	—	Gaussian $\mathcal{N}(30, 64) _{[15, 75]}$
$X_3 = Z_v$	Downstream level	m	Triangular $\mathcal{T}(49, 50, 51)$
$X_4 = Z_m$	Upstream level	m	Triangular $\mathcal{T}(54, 55, 56)$
$X_5 = H_d$	Dyke height	m	Uniform $\mathcal{U}(7, 9)$
$X_6 = C_b$	Bank height	m	Triangular $\mathcal{T}(55, 55.5, 56)$
$X_7 = L$	River length	m	Triangular $\mathcal{T}(4990, 5000, 5010)$
$X_8 = B$	River width	m	Triangular $\mathcal{T}(295, 300, 305)$

TABLE 2. Input variables for the flood model. The notation $|_I$ means that the distribution is truncated on the interval I .

The pdf of the Gumbel distribution $\mathcal{G}(\eta, \beta)$ ($\eta \in \mathbb{R}$, $\beta > 0$) and of the triangular distribution $\mathcal{T}(a, c, b)$ ($a < c < b$) are given respectively by:

$$\rho(x) = \frac{1}{\beta} \exp\left(-\frac{x-\eta}{\beta} - \exp\left(-\frac{x-\eta}{\beta}\right)\right), \quad x \in \mathbb{R},$$

$$\rho(x) = \frac{2(x-a)}{(b-a)(c-a)} \mathbb{1}_{[a,c]}(x) + \frac{2(b-x)}{(b-a)(b-c)} \mathbb{1}_{(c,b]}(x), \quad x \in \mathbb{R}.$$

For the sake of comparison, we need the total Sobol indices and the main effects. Since closed form expressions can be hardly obtained, we estimate them with a large sample of size 10 000 and refer to these estimations as “true” values. More precisely, the total Sobol indices are computed with the function `soboljansen` from the package `sensitivity` [17] and the main effects are estimated with the function `loess` (package `stats`).

We present the results for S and C at the same time, focusing on the variables Q , K_s , Z_v and H_d , which are found to be the most influential. Figure 11 displays the upper bounds. We see that for each variable X_i , the bounds provided by the data-driven weight \widehat{w}_i and $w_{i,\text{lin}}$ are sharp and somewhat similar, except for H_d in the output C , where the bounds are rather rough. This poor result for H_d may be due to the fact that its main effect has a non-monotonic quadratic shape (see Figure 12). Recall that when the main effect is non monotonic, the data-driven weight can be constructed but does not come with a theoretical guarantee. Furthermore, this may cause numerical troubles. For instance, we could not use the SCAM estimator as it produces a flat curve in the region $H_d < 8$ which creates a singularity in the definition of the estimated weight given in (4.5). We have replaced it by an increasing piecewise affine function with knots $H_d = 7, 8, 9$.

We present now the PoinCE approximations in Figures 13 and 14. We obtain relevant and similarly accurate approximations for each variable. This includes the case of the variable H_d in the output C , where no accurate upper bound was provided. This is remarkable, considering that only few basis functions have been

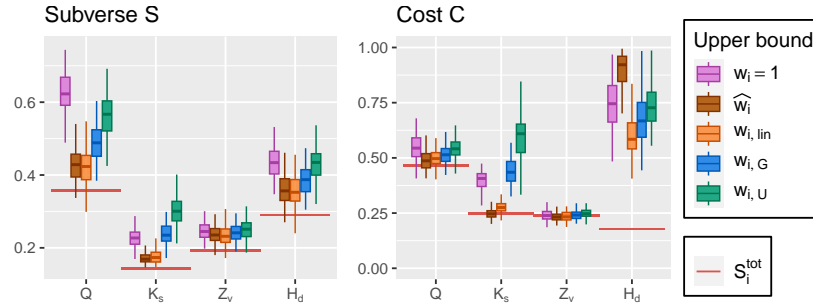


FIGURE 11. Upper bounds of the total Sobol indices for the flood model. Horizontal red bars indicate the true values.

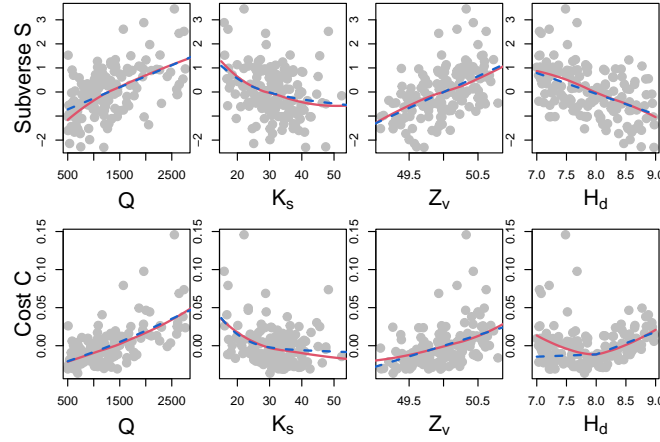


FIGURE 12. Estimators \hat{f}_i (blue lines) of the main effects f_i (red lines) for the recentered outputs of the flood model.

used in the PoinCE chaos. Using more basis functions would reduce the slight bias for the output C .

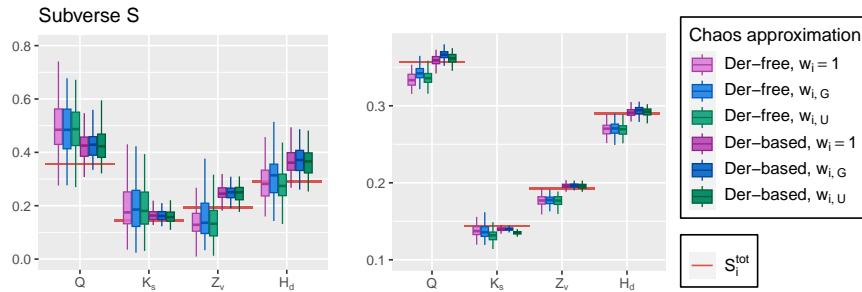


FIGURE 13. PoinCE approximations, estimated with samples of sizes 150 (left) and 10000 (right), of the total Sobol indices for S . Horizontal red bars indicate the true values.

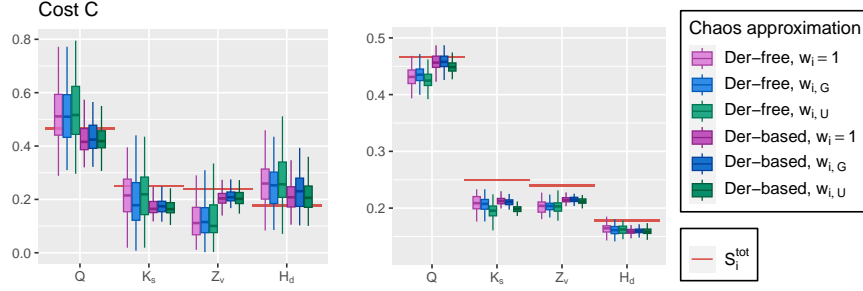


FIGURE 14. PoinCE approximations, estimated with samples of sizes 150 (left) and 10 000 (right), of the total Sobol indices for the flood model (cost output). Horizontal red bars indicate the true values.

ACKNOWLEDGEMENT

This research was supported by the ANR LabEx CIMI *Global sensitivity analysis and Poincaré inequalities* (grant ANR-11-LABX-0040) within the French State Programme “Investissements d’Avenir”.

APPENDIX A.

This short appendix presents the various computations of the weight w_{lin} for each example listed in Table 1. We deal only with the truncated measures, as the weights in the non truncated case are immediately recovered by letting the truncation boundaries tend to infinity. Given some probability measure $\mu \in \mathcal{P}(a, b)$, recall that by Theorem 3.1 the weight w_{lin} is given by

$$w_{\text{lin}}(x) = \frac{1}{\rho(x)} \int_a^x (m - y) \rho(y) dy, \quad x \in [a, b],$$

where m denotes the mean $m = \int_a^b z \rho(z) dz$ and ρ is the Lebesgue density of the measure μ .

Uniform distribution $\mathcal{U}(a, b)$

For all $x \in [a, b]$,

$$w_{\text{lin}}(x) = \frac{a+b}{2} \int_a^x dy - \int_a^x y dy = \frac{1}{2}(x-a)(b-x).$$

Truncated exponential distribution $\mathcal{E}(\gamma)|_{[0,h]}$

In this case the mean is

$$m = \left(\int_0^h \gamma e^{-\gamma z} dz \right)^{-1} \int_0^h \gamma z e^{-\gamma z} dz = \frac{1}{\gamma} - \frac{he^{-\gamma h}}{1 - e^{-\gamma h}},$$

and for all $x \in [0, h]$,

$$\begin{aligned} w_{\text{lin}}(x) &= e^{\gamma x} \left(\left(\frac{1}{\gamma} - \frac{h e^{-\gamma h}}{1 - e^{-\gamma h}} \right) \int_0^x e^{-\gamma y} dy - \int_0^x y e^{-\gamma y} dy \right) \\ &= e^{\gamma x} \left(\left(\frac{1}{\gamma} - \frac{h e^{-\gamma h}}{1 - e^{-\gamma h}} \right) \frac{1}{\gamma} (1 - e^{-\gamma x}) + \frac{1}{\gamma} x e^{-\gamma x} - \frac{1}{\gamma^2} (1 - e^{-\gamma x}) \right) \\ &= \frac{1}{\gamma} \left(x - h \frac{e^{\gamma x} - 1}{e^{\gamma h} - 1} \right). \end{aligned}$$

Truncated normal distribution $\mathcal{N}(m, \sigma^2)|_{[m-h, m+h]}$

For all $x \in [m - h, m + h]$,

$$\begin{aligned} w_{\text{lin}}(x) &= e^{(x-m)^2/2\sigma^2} \int_{m-h}^x (m-y) e^{-(y-m)^2/2\sigma^2} dy \\ &= \sigma^2 e^{(x-m)^2/2\sigma^2} \left(e^{-(x-m)^2/2\sigma^2} - e^{-h^2/2\sigma^2} \right) \\ &= \sigma^2 \left(1 - e^{((x-m)^2 - h^2)/2\sigma^2} \right). \end{aligned}$$

Truncated generalized Cauchy distribution $\mathcal{C}(\beta)|_{[-h, h]}$

We have $m = 0$ and for all $x \in [-h, h]$,

$$\begin{aligned} w_{\text{lin}}(x) &= -(1+x^2)^\beta \int_{-h}^x y (1+y^2)^{-\beta} dy \\ &= \begin{cases} \frac{1}{2(\beta-1)} \left((1+x^2) - (1+x^2)^\beta (1+h^2)^{-\beta+1} \right) & \text{if } \beta \neq 1; \\ -\frac{1}{2} (1+x^2) \log \left(\frac{1+x^2}{1+h^2} \right) & \text{if } \beta = 1. \end{cases} \end{aligned}$$

Truncated Pareto distribution $\mathcal{P}ar(z, \alpha)|_{[z, z+h]}$

• Case $\alpha \neq 1$: the mean is

$$m = \frac{\alpha}{z^{-\alpha} - (z+h)^{-\alpha}} \int_z^{z+h} y^{-\alpha} dy = \frac{\alpha}{\alpha-1} \frac{z^{1-\alpha} - (z+h)^{1-\alpha}}{z^{-\alpha} - (z+h)^{-\alpha}},$$

and for all $x \in [z, z+h]$,

$$\begin{aligned} w_{\text{lin}}(x) &= x^{\alpha+1} \left(m \int_z^x y^{-(\alpha+1)} dy - \int_z^x y^{-\alpha} dy \right) \\ &= x^{\alpha+1} \left(\frac{m}{\alpha} (z^{-\alpha} - x^{-\alpha}) - \frac{1}{\alpha-1} (z^{1-\alpha} - x^{1-\alpha}) \right) \\ &= \frac{x^{\alpha+1}}{\alpha-1} \left(\frac{z^{1-\alpha} - (z+h)^{1-\alpha}}{z^{-\alpha} - (z+h)^{-\alpha}} (z^{-\alpha} - x^{-\alpha}) - (z^{1-\alpha} - x^{1-\alpha}) \right). \end{aligned}$$

• Case $\alpha = 1$: we have $m = (\log(z+h) - \log(z))/(z^{-1} - (z+h)^{-1})$ and for all $x \in [z, z+h]$,

$$\begin{aligned} w_{\text{lin}}(x) &= x^2 \left(m \int_z^x y^{-2} dy - \int_z^x y^{-1} dy \right) \\ &= x^2 \left((\log(z+h) - \log(z)) \frac{z^{-1} - x^{-1}}{z^{-1} - (z+h)^{-1}} - (\log(x) - \log(z)) \right). \end{aligned}$$

REFERENCES

- [1] B. Adcock and Y. Sui. Compressive Hermite Interpolation: Sparse, High-Dimensional Approximation from Gradient-Augmented Measurements. *Constr. Approx.*, 50:167–207, 2007.
- [2] D. Bakry, I. Gentil and M. Ledoux. *Analysis and geometry of Markov diffusion operators*. Grundlehren der mathematischen Wissenschaften, 348, Springer, Heidelberg, 2013.
- [3] F. Barthe, C. Bianchini and A. Colesanti. Isoperimetric bounds and stability of hyperplanes for product probability measures. *Ann. Mat. Pura Appl.*, 192:165–190, 2013.
- [4] S.G. Bobkov and F. Götze. Exponential integrability and transportation cost related to logarithmic Sobolev inequalities. *J. Funct. Anal.*, 163:1–28, 1999.
- [5] S.G. Bobkov and F. Götze. Hardy type inequalities via Riccati and Sturm-Liouville equations. *Sobolev spaces in mathematics*, I:69–86, International Mathematical Series, 8. Springer, New York, 2009.
- [6] S.G. Bobkov and M. Ledoux. Poincaré’s inequalities and Talagrand’s concentration phenomenon for the exponential distribution. *Probab. Theory Relat. Fields*, 107:383–400, 1997.
- [7] S.G. Bobkov and M. Ledoux. Weighted Poincaré-type inequalities for Cauchy and other convex measures. *Ann. Probab.*, 37:403–427, 2009.
- [8] M. Bonnefont and A. Joulin. Intertwining relations for one-dimensional diffusions and application to functional inequalities. *Pot. Anal.*, 41:1005–1031, 2014.
- [9] M. Bonnefont, A. Joulin and Y. Ma. A note on spectral gap and weighted Poincaré inequalities for some one-dimensional diffusions. *ESAIM Probab. Stat.*, 20:18–29, 2016.
- [10] H.J. Brascamp and E.H. Lieb. On extensions of the Brunn-Minkovski and Prékopa-Leindler theorems, including inequalities for log-concave functions and with an application to the diffusion equation. *J. Funct. Anal.*, 22:366–389, 1976.
- [11] R.L. Burden, J.D. Faires and A.M Burden. *Numerical Analysis*. Tenth edition. Cengage Learning, 2015.
- [12] M.F. Chen and F.Y. Wang. Estimation of spectral gap for elliptic operators. *Trans. Am. Math. Soc.*, 349:1239–1267, 1997.
- [13] T. Cui, X. Tong and O. Zahm. Optimal Riemannian metric for Poincaré inequalities and how to ideally precondition Langevin dynamics. Preprint arXiv:2404.02554, 2024.
- [14] M. Ernst, G. Reinert, Y. Swan. First-order covariance inequalities via Stein’s method. *Bernoulli*, 26:2051–2081, 2020.
- [15] G. Germain and Y. Swan. A note on one-dimensional Poincaré inequalities by Stein-type integration. *Bernoulli*, 29:1714–1740, 2023.
- [16] B. Iooss and P. Lemaître. A review on global sensitivity analysis methods. In *Uncertainty management in Simulation-Optimization of Complex Systems: Algorithms and Applications*, C. Meloni and G. Dellino (eds), Springer, 2015.
- [17] B. Iooss, S. Da Veiga, A. Janon, and G. Pujol. sensitivity: Global Sensitivity Analysis of Model Outputs. R package version 1.29.0, 2023. Available at: <https://CRAN.R-project.org/package=sensitivity>.

- [18] S. Da Veiga, F. Gamboa, B. Iooss and C. Prieur. Basics and trends in sensitivity analysis: Theory and practice in R. Society for Industrial and Applied Mathematics, 2021.
- [19] M. Lamboni, B. Iooss, A.-L. Popelin and F. Gamboa. Derivative-based global sensitivity measures: general links with Sobol indices and numerical tests. *Math. Comput. Simulat.*, 87:45-54, 2013.
- [20] A. F. López-Lopera, F. Bachoc, N. Durrande, J. Rohmer, D. Idier, and O. Roustant. Approximating Gaussian Process Emulators with Linear Inequality Constraints and Noisy Observations via MC and MCMC. In: Monte Carlo and Quasi-Monte Carlo Methods. *Springer Int. Publ.* 363–381, 2020.
- [21] N. Lüthen, O. Roustant, F. Gamboa, B. Iooss, S. Marelli and B. Sudret. Global sensitivity analysis using derivative-based sparse Poincaré chaos expansions. *Int. J. Uncertain. Quantif.*, 13:57-82, 2023.
- [22] B. Muckenhoupt. Hardy’s inequality with weights. *Stud. Math.*, 44:31-38, 1972.
- [23] N. Neumeier. A note on uniform consistency of monotone function estimators. *Stat. Probab. Lett.*, 77:693-703, 2007.
- [24] F. W. J. Olver, A. B. Olde Daalhuis, D. W. Lozier, B. I. Schneider, R. F. Boisvert, C. W. Clark, B. R. Miller, B. V. Saunders, H. S. Cohl and M. A. McClain (Eds.). *NIST Digital Library of Mathematical Functions*. Release 1.2.1. National Institute of Standards and Technology, 2024. Available online at <https://dlmf.nist.gov/>.
- [25] N. Pya and S.N. Wood. Shape constrained additive models. *Comput. Stat.*, 25:543–559, 2015.
- [26] O. Roustant, F. Barthe and B. Iooss. Poincaré inequalities on intervals - application to sensitivity analysis. *Electron. J. Statist.*, 11:3081-3119, 2017.
- [27] O. Roustant, F. Gamboa and B. Iooss. Parseval inequalities and lower bounds for variance-based sensitivity indices. *Electron. J. Stat.*, 14:386-412, 2020.
- [28] R Core Team. R: A Language and Environment for Statistical Computing. R Foundation for Statistical Computing, Vienna, Austria, 2023. Available at: <https://www.R-project.org/>.
- [29] A. Saumard. Weighted Poincaré inequalities, concentration inequalities and tail bounds related to Stein kernels in dimension one. *Bernoulli*, 25:3978-4006, 2019.
- [30] K. Soetaert, T. Petzoldt, and R. W. Setzer. Solving Differential Equations in R: Package deSolve. *J. Stat. Softw.*, 33(9):1–25, 2010.
- [31] I.M. Sobol. Sensitivity estimates for non linear mathematical models. *Mathematical Modelling and Computational Experiments*, 1:407-414, 1993.
- [32] I.M. Sobol. Global sensitivity indices for nonlinear mathematical models and their Monte Carlo estimates. *Math. Comput. Simulat.*, 55:271-280, 2001.
- [33] I.M. Sobol and S. Kucherenko. Derivative-based global sensitivity measures and the link with global sensitivity indices. *Math. Comput. Simulat.*, 79:3009-3017, 2009.
- [34] I.M. Sobol and S. Kucherenko. A new derivative based importance criterion for groups of variables and its link with the global sensitivity indices. *Comput. Phys. Commun.*, 181:1212-1217, 2010.
- [35] S. Song, Z. Tong, L. Wang, S. Kucherenko and Z. Lu. Derivative-based new upper Bound of Sobol’ sensitivity measure. *Reliab. Eng. Syst. Saf.*, 187:142-148, 2018.

- [36] A. Zettl. *Sturm-Liouville Theory*. Mathematical Surveys and Monographs, 121, American Mathematical Society, Providence, 2005.

(D. Heredia, corresponding author) UMR CNRS 5219, INSTITUT DE MATHÉMATIQUES DE TOULOUSE, UNIVERSITÉ DE TOULOUSE, FRANCE

E-mail address: <mailto:dheredia@insa-toulouse.fr>

URL: <https://davidherediag.wordpress.com/>

(A. Joulin) UMR CNRS 5219, INSTITUT DE MATHÉMATIQUES DE TOULOUSE, UNIVERSITÉ DE TOULOUSE, FRANCE

E-mail address: <mailto:ajoulin@insa-toulouse.fr>

URL: <https://perso.math.univ-toulouse.fr/joulin/>

(O. Roustant) UMR CNRS 5219, INSTITUT DE MATHÉMATIQUES DE TOULOUSE, UNIVERSITÉ DE TOULOUSE; INSA TOULOUSE, FRANCE.

E-mail address: <mailto:roustant@insa-toulouse.fr>

URL: <https://olivier-roustant.fr/>